PRIMER

Parallel nuclear magnetic resonance spectroscopy

Ēriks Kupče[1] ✉, *Lucio Frydman*[2], *Andrew G. Webb*[3], *Jonathan R. J. Yong*[4] and *Tim D. W. Claridge*[4]

Abstract | Nuclear magnetic resonance (NMR) spectroscopy is a principal analytical technique used for the structure elucidation of molecules. This Primer covers different approaches to accelerate data acquisition and increase sensitivity of NMR measurements through parallelization, enabled by hardware design and/or pulse sequence development. Starting with hardware-based methods, we discuss coupling multiple detectors to multiple samples so each detector/sample combination provides unique information. We then cover spatio-temporal encoding, which uses magnetic field gradients and frequency-selective manipulations to parallelize multidimensional acquisition and compress it into a single shot. We also consider the parallel manipulation of different magnetization reservoirs within a sample to yield new, information-rich pulse schemes using either homonuclear or multinuclear detection. The Experimentation section describes the set-up of parallel NMR techniques. Practical examples revealing improvements in speed and sensitivity offered by the parallel methods are demonstrated in Results. Examples of use of parallelization in small-molecule analysis are discussed in Applications, with experimental constraints addressed under the Limitations and optimizations and Reproducibility and data deposition sections. The most promising future developments are considered in the Outlook, where the largest gains are expected to emerge once the discussed techniques are combined.

Precessional
The process by which nuclei spins rotate (precess) about an applied magnetic field.

Gradient-based spatial encoding
Selective excitation in the presence of magnetic field gradients.

[1]*Research and Development, Bruker UK Ltd, Coventry, UK.*

[2]*Department of Chemical and Biological Physics, Weizmann Institute of Science, Rehovot, Israel.*

[3]*Department of Radiology, Leiden University Medical Center, Leiden, Netherlands.*

[4]*Chemistry Research Laboratory, Department of Chemistry, University of Oxford, Oxford, UK.*

✉*e-mail: eriks.kupce@bruker.com*

https://doi.org/10.1038/s43586-021-00024-3

The separation of a large task into multiple segments that can be tackled simultaneously has been exploited in many fields of science and technology. For example, parallel genome sequencing has reduced the long-term cost and increased throughput by more than three orders of magnitude[1]. Similar developments in magnetic resonance imaging (MRI) have provided great increases in sensitivity and faster image acquisition[2–4] via multiple receiver coils and detector channels. In MRI, an image is formed from the water protons in tissue, with magnetic field gradients being applied to impose a unique combination of precessional phase and frequency at each position within the image. By using multiple receiver coils, the unique spatial profiles of each of the coils can be used to reduce the requirements for gradient-based spatial encoding, enabling under-sampling of reciprocal space and increasing the imaging speed without compromising the image quality. These examples have served as the inspiration for similar techniques in nuclear magnetic resonance (NMR) spectroscopy, which we broadly term parallel NMR spectroscopy.

NMR spectroscopy, in its simplest form, is the measurement of energy differences between spin states of nuclei with non-zero spin induced by external or internal magnetic fields. Owing to differences in their surrounding chemical environments, each nucleus in a molecule will have characteristic energy differences, which are often expressed in terms of resonance frequencies or chemical shifts. NMR can also detect magnetic interactions between nuclear spins via either through-bond (scalar) or through-space (dipolar) coupling interactions, which can be directly correlated with molecular structure.

Routine NMR applications typically involve spin-½ nuclei commonly found in organic compounds and biomolecules, such as ^{1}H, ^{13}C, ^{15}N, ^{19}F and ^{31}P. Of these, ^{1}H, ^{19}F and ^{31}P are particularly important as their high natural abundance and magnetogyric ratio (γ) provide greater detection sensitivity. One-dimensional (1D) NMR experiments directly measure the chemical shifts of and couplings between these nuclei, which provide direct information about their chemical environments. More intricate multidimensional (nD) NMR experiments use separate spectral dimensions, usually for correlating different nuclei in a molecule. In an nD pulse sequence, each spectral dimension corresponds to a time period in which chemical shifts and spin–spin couplings are allowed to evolve. These are interspersed with mixing periods that transfer magnetization from one nucleus to other adjacent nuclei. Different forms of mixing

Chemical shifts
The resonant frequencies of a nucleus relative to those of a defined chemical group within a reference compound.

Magnetogyric ratio
(γ). The ratio of the magnetic moment of a nucleus to its angular momentum.

Spectral dimensions
Frequency dimensions in nuclear magnetic resonance spectra that will typically reflect chemical shifts and/or coupling constants.

Mass-limited samples
Samples of limited amount; the term is used to distinguish from the situation of low concentration due to poor solubility. The sensitivity of nuclear magnetic resonance measurements of mass-limited samples can be improved by using small-diameter probes and higher sample concentrations, prompting use of the term 'mass sensitivity' for small-diameter probes.

Phase shift
A change in the phase of a signal or waveform.

Transient
(Also referred to as a scan). The acquisition of a solitary free induction decay.

enable the identification of different forms of molecular connectivity (see BOX 1 for examples). In nD spectra, a total of $n-1$ evolution periods must be independently incremented, leading to long experiment times.

In this Primer, we describe various parallelization techniques that allow the concurrent acquisition of different signals to reduce the time needed for collection of nD NMR data. The small energy differences between nuclear spin states make NMR spectroscopy an inherently low-sensitivity method. We show that the parallelization techniques offer new ways of increasing the sensitivity of NMR experiments.

The first parallel NMR technique covered in this Primer is the use of multiple radiofrequency microcoils in NMR[5]. Microcoils, which have dimensions of a millimetre or less, are typically used for high-sensitivity NMR of mass-limited samples such as small proteins[6]. For parallel NMR, multiple microcoils are fitted within the usable volume of the NMR magnet, and many (different) samples are then inserted in the bore of the NMR magnet. The aim is to use one coil per sample and acquire all sample signals simultaneously. Another mode of operation is to use multiple microcoils on a single sample that has been split into different aliquots, a process that can significantly reduce total data acquisition times in nD NMR spectroscopy. In order to process the data from separate coils, they must first be aligned in time by a suitable phase shift and then any slight differences in coil sensitivity corrected by normalization.

This concept of physically separating a sample into subsamples studied by individual coils has a natural link to the next parallel technique, spatially encoded ultra-fast NMR. In ultra-fast NMR experiments, the sample is effectively sectioned using magnetic field gradients[7–11], which spread the frequencies of the spins in the sample according to their physical positions. When combined with frequency-selective pulses, this allows 2D NMR (or pseudo-2D NMR; for example, relaxation, diffusion) experiments to be performed in a single transient instead of multiple scans with different time increments. The ultra-fast approach to 2D NMR thus endows different spatial 'bins' with what amounts to different time evolutions. This 'binning' manipulation can be executed in a single shot and is compatible with either homonuclear or heteronuclear 2D correlation pulse sequences (COSY, TOCSY, HSQC, HMQC; see also BOX 1). Thus, ultra-fast NMR enables the collection of complete nD NMR spectral sets with time frames orders of magnitude shorter than conventional techniques, and couples well with measurements that are incompatible with prolonged acquisition times, such as experiments involving hyperpolarized nuclear states in dynamic nuclear polarization[12].

The introduction of multiple receivers in NMR spectroscopy, also adopted from MRI, has led to the development of new types of experiment involving simultaneous detection of free induction decays (FIDs) from several nuclear species[13]. This allows the design of more efficient pulse schemes and supersequences. Furthermore, experiments with simultaneous detection of high-abundance, high γ nuclei, such as ^{1}H and ^{19}F, double the amount of detected signal in direct and indirect detection experiments and improve the sensitivity per unit of measurement time[14].

Finally, we describe recent approaches to data acquisition that provide time-efficient 2D NMR data collection by strategically sampling separate pools of magnetization available within samples while storing others for subsequent collection in the same experiment[15,16]. This tailored sampling of magnetization reservoirs manipulated in parallel yields multiple 2D data sets from a single experiment. One parallelized experiment can thus provide a complete set of through-bond and through-space correlations within molecular structures, which may then be combined to yield complete molecular connectivity and 3D structures. We describe various approaches to parallelized sampling that use the direct acquisition of proton magnetization reservoirs for maximum sensitivity and that can be collected using conventional spectrometer hardware. These include time-shared experiments, experiments that exploit differing magnetization transfer pathways and the modular NOAH supersequences. The time efficiency of the methods will be exemplified by the elucidation of complete structures from single multi-FID experiments.

All of the aforementioned examples of NMR parallelization serve to greatly reduce data acquisition times, which can frequently be translated into associated gains in sensitivity per unit time. Along with the fundamental concepts of each of these techniques, we show selected examples of obtained spectra and consider their application in various contexts where NMR is already used routinely. We end by briefly covering a few key points about experiment reproducibility, limitations and potential avenues for future improvement.

Experimentation

Generally, NMR is considered to be a low-sensitivity technique. The two main approaches to tackle this problem are improvements in instrumentation and methodology developments. Parallelization of NMR involves both of

Box 1 | Basic 2D NMR experiments

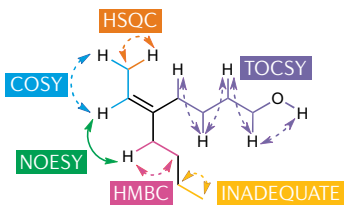

Two-dimensional (2D) nuclear magnetic resonance (NMR) pulse sequences generally follow a 'preparation–evolution–mixing–detection' scheme (see Eq. 2). Processing of the recorded data (Fourier transformation of both frequency domains) leads to cross-peaks in the 2D spectrum at (ω_1, ω_2) that correlate the spin interactions of the two nuclei. Experiments differ according to the nature of the mixing process employed, which is commonly designed to reveal through-bond (scalar) or through-space (dipolar) spin coupling interactions between nuclei. Some examples of classes of 2D experiments are summarized below.

- COSY: correlates mutually scalar coupled (*J*-coupled) ^{1}H spins
- NOESY and ROESY: identifies ^{1}H spins that are close in space (typically <5 Å) and, hence, share dipolar coupling
- TOCSY: distributes magnetization within a ^{1}H spin system to identify a group of mutually scalar coupled protons
- HSQC and HMQC: heteronuclear experiments that typically link an insensitive nucleus (such as ^{13}C or ^{15}N) with directly attached protons
- HMBC: heteronuclear experiments that correlate an insensitive nucleus (such as ^{13}C or ^{15}N) with protons that are remote in a molecular structure (typically within two or three bonds)
- INADEQUATE: correlates scalar coupling between insensitive nuclei (usually ^{13}C)

COSY
(Correlation spectroscopy). A technique for identifying directly scalar coupled (*J*-coupled) nuclei, most often protons.

TOCSY
(Total correlation spectroscopy). A technique related to COSY that distributes magnetization within a network of mutually scalar coupled protons so as to group them within a structure.

HSQC
(Heteronuclear single-quantum correlation). An experiment used to correlate an insensitive nucleus (such as ^{13}C or ^{15}N) with its directly attached proton(s) via one-bond scalar coupling.

HMQC
(Heteronuclear multiple-quantum correlation). An experiment closely related to HSQC and HMBC used to correlate an insensitive nucleus (such as ^{13}C or ^{15}N) with its directly attached proton(s) via one-bond scalar coupling.

Dynamic nuclear polarization
A technique that uses unpaired electron spins to boost the nuclear magnetic resonance signal by as much as 100,000.

Free induction decays
(FIDs). The observable nuclear magnetic resonance signals generated by non-equilibrium nuclear spin magnetization precessing about the magnetic field.

Supersequences
Sequences of nuclear magnetic resonance experiments (pulse schemes) with a common relaxation delay.

Pools of magnetization
Subsets of nuclear spins, typically defined by their coupling interactions with other nuclear magnetic resonance-active spins.

NOAH
(Nuclear magnetic resonance by ordered acquisition using ^{1}H detection). An experimental scheme for acquiring multiple experiments in one but requiring only a single relaxation delay.

Polarization transfer
The transfer of nuclear polarization between subsets of nuclear spins.

these approaches. We therefore start this section by briefly introducing the sensitivity aspects of NMR measurements, focusing on NMR probes. This is followed by instrumentation used in parallel NMR, such as probes with multiple microcoils, and systems with multiple receivers. We then describe experimental set-ups and essential considerations for parallelization methods based on simultaneous detection of multiple FIDs, spatio-temporal encoding and ultra-fast NMR spectroscopy.

NMR probes and sensitivity

The sensitivity of routine NMR experiments largely depends on the available probe configurations and the magnetic field strength (B_0). Nuclei with high γ and high natural abundance (^{1}H, ^{19}F, ^{31}P) offer the highest sensitivity, whereas magnetically diluted and low γ spins (^{13}C, ^{15}N, ^{29}Si) are typically observed indirectly, via high γ abundant nuclei (see TABLE 1). In experiments involving polarization transfer between nuclei, the signal to noise ratio (*S*/*N*) can be defined as follows:

$$S/N \propto n\gamma_e\sqrt{\gamma_d^3 B_0^3 T_{exp}} \quad (1)$$

where n is the number of observed spins, T_{exp} is the experiment time, γ_e and γ_d are magnetogyric ratios of the excited and detected spins, respectively, and B_0 is the magnetic field strength[17,18]. The highest commercially available B_0 value suitable for NMR is currently 28.2 T, corresponding to a ^{1}H resonance frequency of 1.2 GHz. Larger magnetic fields allow greater sensitivity (Eq. 1) as well as improved peak dispersion in NMR spectra. However, owing to the large cost of purchasing and installing very high-field spectrometers, routine small-molecule experiments are typically conducted using systems of 400–700 MHz.

Cryogenic probes[19], although still expensive, offer a considerably cheaper way to improve the sensitivity of measurements relative to the cost of increasing B_0. In most commercial NMR probes there are typically two nested radiofrequency coils that are tuned to the NMR frequencies of various nuclear species. The sensitivity depends on the probe filling factor (the fraction of the coil's active volume that is filled with sample) and the configuration of the radiofrequency coils. The inner coil is closer to the sample and therefore offers better sensitivity. It is usually tuned to ^{1}H to maximize the sensitivity in most routine experiments. The less sensitive outer coil is used primarily for indirect detection of other nuclear species (the 'hetero nuclei') via pulsing and decoupling. This coil is typically tuneable to either a wide range of frequencies (broadband probes) or a set of two or three fixed resonance frequencies of the most commonly observed nuclei in organic molecules and biomolecules, such as ^{13}C, ^{15}N, ^{19}F or ^{31}P. Indirect detection cryoprobes, for example, are tuned to ^{1}H (inner coil) and ^{13}C and ^{15}N (outer coil). In direct detection probes, the coil configuration is reversed to maximize the sensitivity of experiments involving direct detection of hetero nuclei.

Probes dedicated to detection of a single nuclear species, such as cryoprobes optimized for ^{13}C detection, offer the highest sensitivity. Larger diameter probes accommodating increasing sample volumes increase n in Eq. 1 and result in further improvement of *S*/*N*, with direct detection probes designed for sample tubes of diameter 10 mm, 8 mm and, most commonly, 5 mm. Small-diameter probes can significantly reduce the amount of sample necessary for measurements, thereby increasing the sensitivity of mass-limited samples[20]. For example, on a 600-MHz instrument equipped with a 1.7-mm inverse detection cryoprobe, 10 µg of substance is sufficient for detecting ^{13}C–^{15}N correlations at the natural abundance of isotopes (approximately one ^{13}C–^{15}N pair in 25,000 molecules)[21]. Likewise, the 3D structure of a protein has been determined using a 6 µl sample of 1.4 mM 68-residue protein and a 1-mm microcoil NMR probe[22].

Table 1 | **NMR properties of the most commonly observed nuclei**[18]

Nucleus	γ (MHz/Tesla)	Natural abundance (%)	Relative sensitivity
^{1}H	42.58	99.98	1.00
^{13}C	10.71	1.11	1.76×10^{-4}
^{15}N	–4.32	0.37	3.85×10^{-6}
^{19}F	40.08	100.0	0.83
^{29}Si	–8.46	4.7	3.69×10^{-4}
^{31}P	17.25	100.0	6.65×10^{-2}

NMR, nuclear magnetic resonance.

For low-concentration samples, sensitivity is a crucial issue, and typically a large number of transients are required to obtain spectra of acceptable quality. In this sensitivity-limited regime, parallelized experiments are useful only when a gain in sensitivity per unit time can be achieved, as this means that less time is required to reach the *S*/*N* threshold. In this respect, it is important to note that the sampling of indirect domains in *n*D NMR experiments involves a sort of signal averaging — a summation that becomes evident upon performing the full Fourier analysis of the data. On the other hand, the primary constraint for more concentrated samples is spectral resolution, particularly in indirect dimensions. In this resolution-limited regime, the time savings afforded by parallelized experiments can be fully exploited, as any moderate decreases in *S*/*N* resulting from the shorter experiments are easily tolerated. For mass-limited samples, high detection sensitivity will therefore prove to be advantageous as this allows one to move from the sensitivity-limited to the resolution-limited regime, with probes optimized for proton detection and/or cryogenic probes being the most beneficial.

NMR with multiple microcoils

There are two hardware-enabled approaches to parallel NMR with multiple microcoils: the first uses multiple coils that are connected in parallel, with the combination being impedance-matched by a single electronic circuit and fed into a single receiver via a single coaxial cable to the NMR spectrometer (FIG. 1). This has the advantage of electrical simplicity, but as noise for microcoils is coil-dominated, the overall noise contribution is higher than that for a single microcoil. In a parallel configuration, the signals from each sample are separated through the use of spatially selective pulse sequences

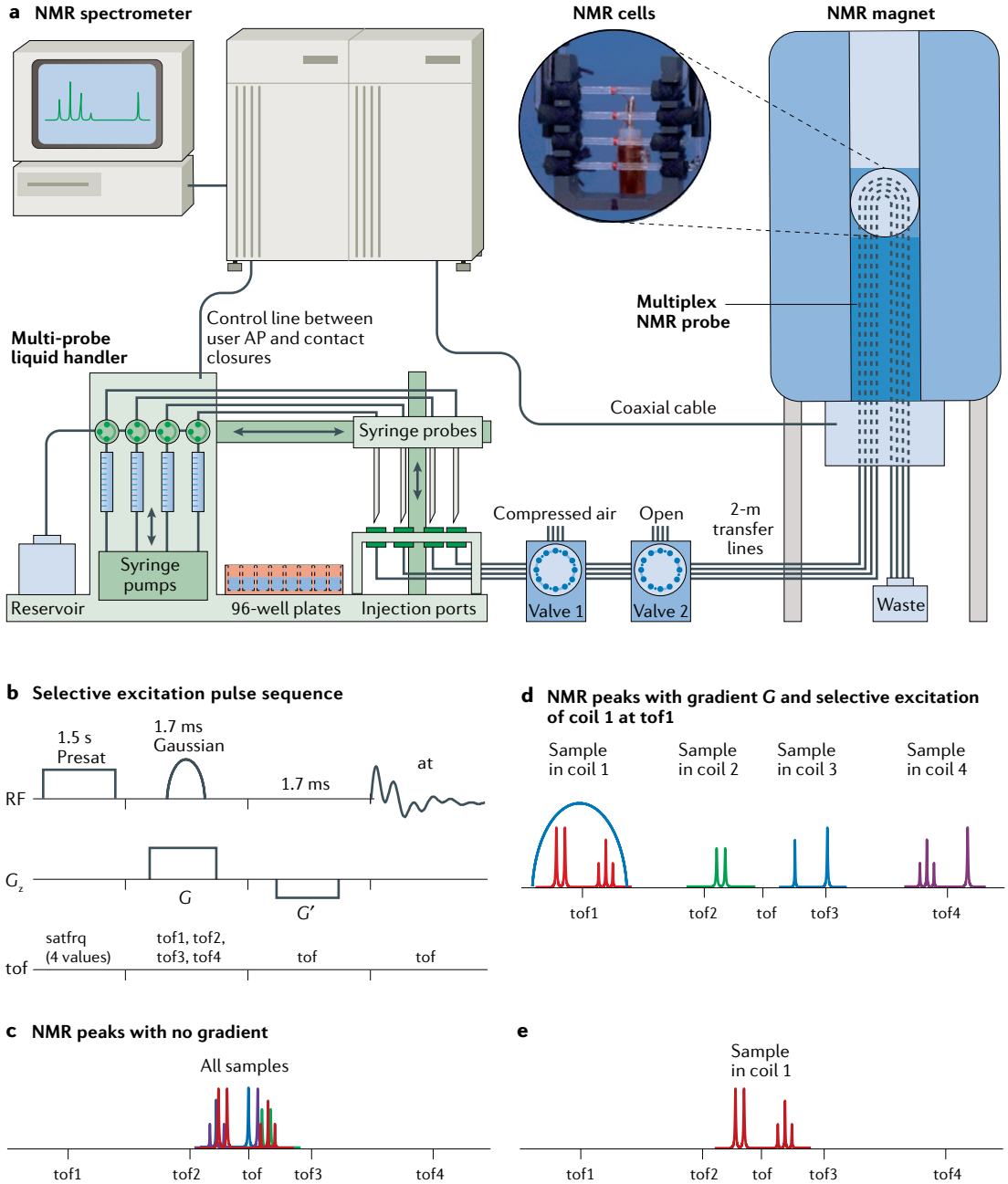

Fig. 1 | **Approach to multiple microcoil NMR using radiofrequency coils connected in parallel. a** | In this configuration, data from multiple samples are acquired in a single experiment using a spatially selective pulse — a frequency-selective pulse applied simultaneously with a magnetic field gradient in the *z* direction — akin to slice selection in magnetic resonance imaging (MRI). **b** | Spatially selective excitation pulse sequence. **c** | Nuclear magnetic resonance (NMR) spectrum with no gradient. **d** | NMR spectra from all samples separated with gradient *G* and selective excitation of individual coils with transmitter offsets tof1–tof4. **e** | NMR spectrum recorded with coil 1. AP, applications panel; at, acquisition time; RF, radiofrequency; satfrq, saturation frequency. Adapted with permission from REF.[24], ACS.

using a frequency-selective pulse[23–26]. The sequence shown in FIG. 1b used to acquire the data employs a frequency-selective Gaussian pulse: the frequency offset of this pulse selects one of the four samples shown in the inset of FIG. 1a. If a conventional hard pulse is used, then the signals from all of the samples are acquired at once (FIG. 1c). By selecting only the relevant frequency range (FIG. 1d), the signal from only one of the samples at a time can be acquired (FIG. 1e).

Approaches using magnetic field gradients in combination with frequency-selective pulses for a single sample in a single coil have been extensively reviewed[27]. These techniques have the advantage of requiring no hardware additional to a standard NMR spectrometer, and in cases where *S*/*N* is high enough these methods can significantly increase the rate of data acquisition, such as for efficient T_1 (longitudinal relaxation time) measurements[28], diffusion ordered

Magnetization helices
Spatially dependent magnetization patterns, where each chemical site's magnetization subtends a helix whose pitch is linearly proportional to the site's chemical shift.

spectroscopy experiments[29] and homonuclear broadband decoupling[30].

The second approach is to separate each of the coils for each to have their own impedance matching circuit, which gives optimal S/N[31–35]. This increases the complexity of the electrical circuitry: although NMR systems may have multiple receive channels, there is typically only one transmit channel for each nucleus, and so pulse transmission must be switched between the coils (FIG. 2). The major challenge with multiple microcoils is to achieve electrical isolation between the coils so that neither signal nor noise is transferred between coils, and to ensure that B_0 is sufficiently homogeneous over each of the samples to achieve high spectral resolution. Provided that the physical separation between coils is sufficiently large compared with the size of the coil, high isolation can be achieved. If this condition is not met, then small shielding conductors can be placed between coils. The B_0 homogeneity is further improved by placing magnetic susceptibility matching fluid around each of the microcoils. This enables one to resolve scalar-coupled multiplets and resonances with close chemical shift values.

There are different types of parallel NMR experiments. The simplest is to run several samples at once, with one sample associated with one microcoil, to increase throughput. Alternatively, a single sample can be split into different aliquots and flowed into each of the detector coils and different sequences, or different components of sequences, run simultaneously. For example, a COSY spectrum might be acquired with coil 1, a TOCSY with coil 2, an HSQC with coil 3 and so on; or the first n time increments in the indirectly detected domain (t_1 increments) of a TOCSY acquired on coil 1, the second n t_1 increments on coil 2 and so on. When the data from all coils are concatenated, they yield a data set with the total number of required t_1 increments acquired in a time reduced by a factor of the number of coils. Both of these types of experiment have been shown using two, four and eight radiofrequency coils, for proton high-resolution spectroscopy of small molecules and multinuclear spectroscopy of small proteins[31–33].

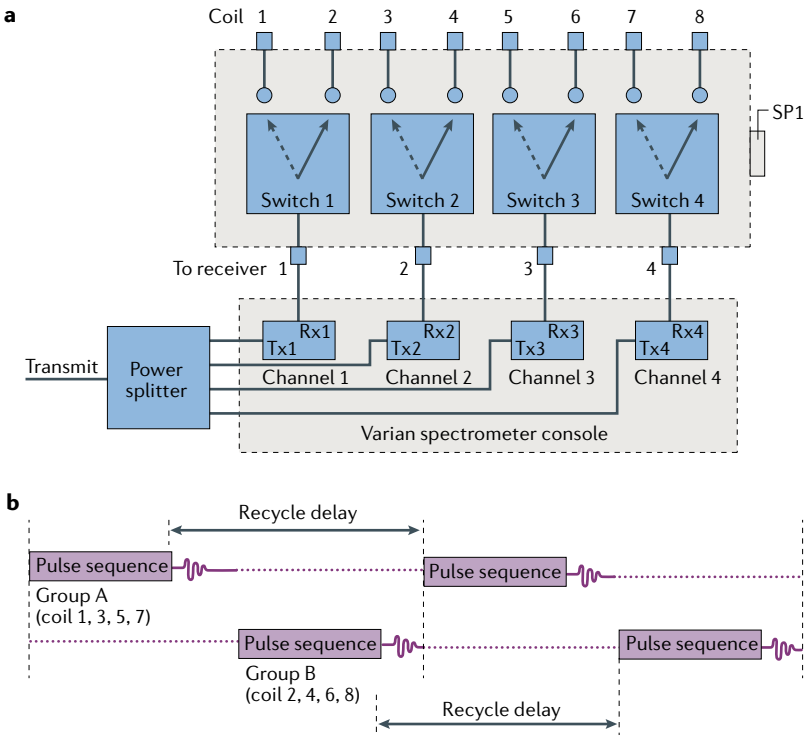

Fig. 2 | **Approach using radiofrequency coils that are electrically and magnetically separate from one another.** Switches 1–4 activated by a trigger signal from a spare port (SP1) are used to rapidly switch between transmitting pulses (Tx1–Tx4) to each of the eight radiofrequency coils (part **a**). The received signals are fed into separate receive channels (Rx1–Rx4). As the probe head contains eight coils but there are only four receivers on the system, an interleaved mode, shown representatively in part **b**, is used to record separate spectra from all eight samples. Adapted with permission from REF.[33], Elsevier.

Single-scan nD NMR

The concept of physically separating a sample into subsamples studied by individual coils can be notionally extended to sectioning a sample into multiple emitters using magnetic field gradients. This is the idea underlying ultra-fast *n*D NMR, where magnetic field gradients and frequency-selective pulses are combined to distinguish different positions within a sample[9,36,37]. This idea is easiest to visualize when considering a 2D NMR acquisition, where $S(t_1,t_2)$ signals are collected within the framework of the Jeener–Ernst classical scheme[38,39]:

$$\text{Relaxation / Preparation–Evolution}(t_1)\text{–Mixing–Detection}(t_2) \quad (2)$$

Here, the preparation and the mixing events remain constant, whereas signals are collected by changing parameter t_1 through a series of independent scans. This leads to a collection of signals depending on two time variables t_1 and t_2. Instead of considering a t_1 time evolution parameter that is incremented scan by scan to monitor the frequencies $I(\Omega_1)$ making up an indirect-domain spectrum, ultra-fast 2D NMR executes the encoding along a spatial direction as illustrated in FIG. 3.

FIGURE 3a shows the classical scheme of a 2D experiment, where the duration of t_1 is changed scan to scan over N_1 increments for all spins in the sample, taken as one homogeneous set. FIGURE 3b shows the spatio-temporally encoded scheme, where different positions along the sample's z-axis B_0 are first endowed with different evolution times as a function of their position within the NMR tube (referred to as the 'encoding' process), and then acquired in a spatially resolved fashion as a function of t_2 (referred to as the 'decoding' process). Ultra-fast 2D NMR executes both the encoding and the decoding processes within a single scan, by using magnetic field gradients. Such fields are used during the evolution to address spins positioned at different z coordinates and impart an evolution time t_1 that is proportional to their positions. As further detailed in Supplementary Experimentation, a unique feature of this kind of spatio-temporal (z/t_1) encoding is the creation of magnetization helices — patterns of magnetization where the pitch of the helices has encoded the indirect-domain interaction. Ultra-fast 2D NMR then uses the echo-planar spectroscopic imaging block[40] over the course of the acquisition to collect the 2D NMR data. Echo-planar spectroscopic imaging views its signal as

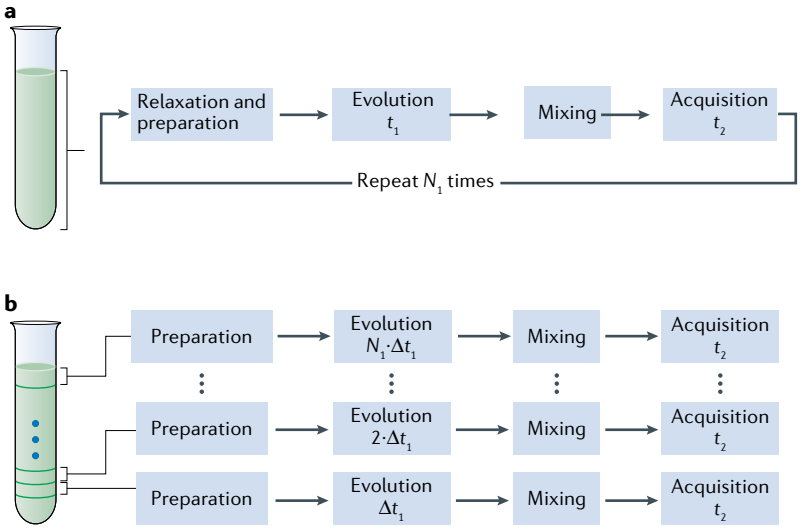

Fig. 3 | **Comparison of data acquisition schemes in conventional versus ultra-fast 2D NMR. a** | Conventional two-dimensional (2D) nuclear magnetic resonance (NMR) experiment. **b** | Ultra-fast single-shot 2D NMR experiment. Although this schematic compares the two experimental techniques by retaining the same nominal number of N_1 elements, the actual ultra-fast experiments are usually performed using continuous spatio-temporal encoding. Processing of the two types of data sets is usually different, even as both approaches lead to the same final spectra. For further details see Supplementary Fig. 1. Adapted with permission from REF.[11], Annual Reviews.

a function of the direct-domain acquisition time t_2, and as a function of variable k:

$$k = \gamma \int_0^{t_2} G_a(t')\mathrm{d}t' \quad (3)$$

where k describes the evolution imposed by a linear magnetic field gradient. This k value oscillates back and forth by periodically reversing the sign of the acquisition gradient G_a; as it does so, it will periodically 'unwind' the aforementioned magnetization helices, leading to echoes that map in a one to one fashion the indirect-domain peak positions and intensities expected from the 2D NMR acquisition. The k axis thus becomes equivalent to the indirect F_1 frequency axis in 2D NMR; as a result of this, there is no need to perform an explicit Fourier transform to retrieve an indirect-domain spectrum that has been spatio-temporally encoded. This type of single-shot 2D acquisition only requires splicing of the single string of data collected over the course of the echo-planar spectroscopic imaging acquisition into a 2D array, rearranging this 2D array into a bidimensional grid according to each data point's $(k/F_1,t_2)$ coordinate and a final 1D Fourier transform along the directly detected t_2 axis to transform these direct time-domain evolutions into frequencies along the second F_2 domain.

This single-scan parallelization of the Jeener–Ernst 2D NMR scheme (Eq. 2) does not need to be circumscribed to one indirect domain: multiple gradients can be used to encode multiple independent dimensions — x, y and z gradients, for instance, have been used simultaneously to coalesce a 4D NMR experiment into a single scan[37]. Furthermore, as long as samples are spatially homogeneous, the same strategy can be used to encode incoherent processes such as spin-lattice relaxation behaviour or diffusivity[27–29,41–43]. Somewhat related to this topic, but outside the bounds of this survey, is the use of gradients and frequency-selective pulses for achieving homonuclear broadband decoupling[30]. Last, but not least, this spatio-temporal encoding strategy arguably sees its most widespread applications in cases of heterogeneous samples, where it has been used to deliver single-shot nD MRI images and nD spectral images with unprecedented speed and robustness[44–49].

Homonuclear multi-FID detection

Biomolecular NMR studies typically involve low-concentration samples (≤1 mM) that are routinely enriched in ^{13}C (natural abundance = 1.1%) and ^{15}N (natural abundance = 0.37%) to improve measurement sensitivity. By contrast, in small-molecule research, more concentrated samples are usually available and sample enrichment is considered too expensive or impractical for routine applications. In this section, we focus on small-molecule NMR, which is typically performed at natural isotopic abundance.

In a given sample, there typically exist multiple magnetization pools that can be manipulated selectively as they originate from different nuclear spins (FIG. 4a). For example, protons directly bound to ^{13}C can be distinguished from other protons on the basis of their large one-bond C–H coupling using pulse sequence elements such as BIRD pulses[50], TANGO/BANGO elements[51,52] or zz filters[53,54]. The development of parallelized nD experiments relies on the concurrent manipulation of multiple magnetization pools such that the respective signals arising from each pool may be detected without the conventional recovery delay (d_1 in FIG. 4) between individual pulse schemes (FIG. 4b). The recovery delay is typically the longest time period in any pulse

Fig. 4 | **Exploiting isotope-specific magnetization.** **a** | Isotopomers of a typical organic molecule illustrating the different magnetization pools present, namely ^{13}C-bound protons (blue), remote ^{13}C-coupled protons (purple), ^{15}N-bound protons (orange) and protons not scalar coupled to heteroatoms (green), which contribute to different correlation spectra. **b** | Conventional (separate) acquisition of the ^{1}H–^{13}C and ^{1}H–^{15}N HSQC and ^{1}H–^{1}H COSY spectra. Each experiment requires a recovery delay (d_1) to allow proton magnetization to relax towards equilibrium before being sampled. **c** | Simultaneous acquisition of both free induction decays (FIDs) using the time-shared principle. The final data set contains two phase-encoded ($\phi = +x$ or $-x$) subsets that are separated at the processing stage (blue and orange). Fourier transformation (FT) of each subset gives a spectrum containing peaks from both ^{15}N-bound and ^{13}C-bound protons, which can be separated via nucleus editing. Only a single recovery delay is required. **d** | Sequential acquisition in a NOAH-style experiment comprising multiple experiment modules indicated using single-letter codes, here the NOAH-4 BMSC (B, HMBC; M, HMQC; S, HSQC; C, COSY). All FIDs are stored in a single two-dimensional (2D) matrix that has been partitioned into memory blocks. Separation of these blocks and FT yield the individual spectra. As with simultaneous acquisition, only a single recovery delay is needed, but far greater flexibility in experiment design is available. H-1, radiofrequency channel corresponding to the nuclei detected.

Echoes
Signals that peak as a function of the k-domain variable, according to their indirect-domain chemical shift.

Recovery delay
(Also known as relaxation delay). A time period in which spins recover their equilibrium populations between scans.

Nucleus editing
Recording multiple data sets in which signals from separate pools are phase-labelled relative to one another.

sequence and significant time can be saved by reducing the number of these delays during data collection. This can be done even on basic desktop spectrometers equipped with only a single receiver and no gradients (see Supplementary Fig. 2).

The signals from each magnetization pool can be collected either simultaneously as part of one FID or sequentially in a multiple-FID experiment. Simultaneous acquisition is exemplified by time-shared experiments[55], in which multiple indirect-dimension frequencies (typically ^{15}N and ^{13}C) are encoded and then transferred back to ^{1}H for detection (FIG. 4c). Each resulting FID is a sum of the component signals, and direct Fourier transformation will yield a spectrum containing signals from every magnetization pool sampled. These signals can be separated using nucleus editing, following which addition and subtraction of the phase-labelled data sets yield spectra containing only one signal[56].

Sequential acquisition is typified by NOAH methods — experiments in which signals from different

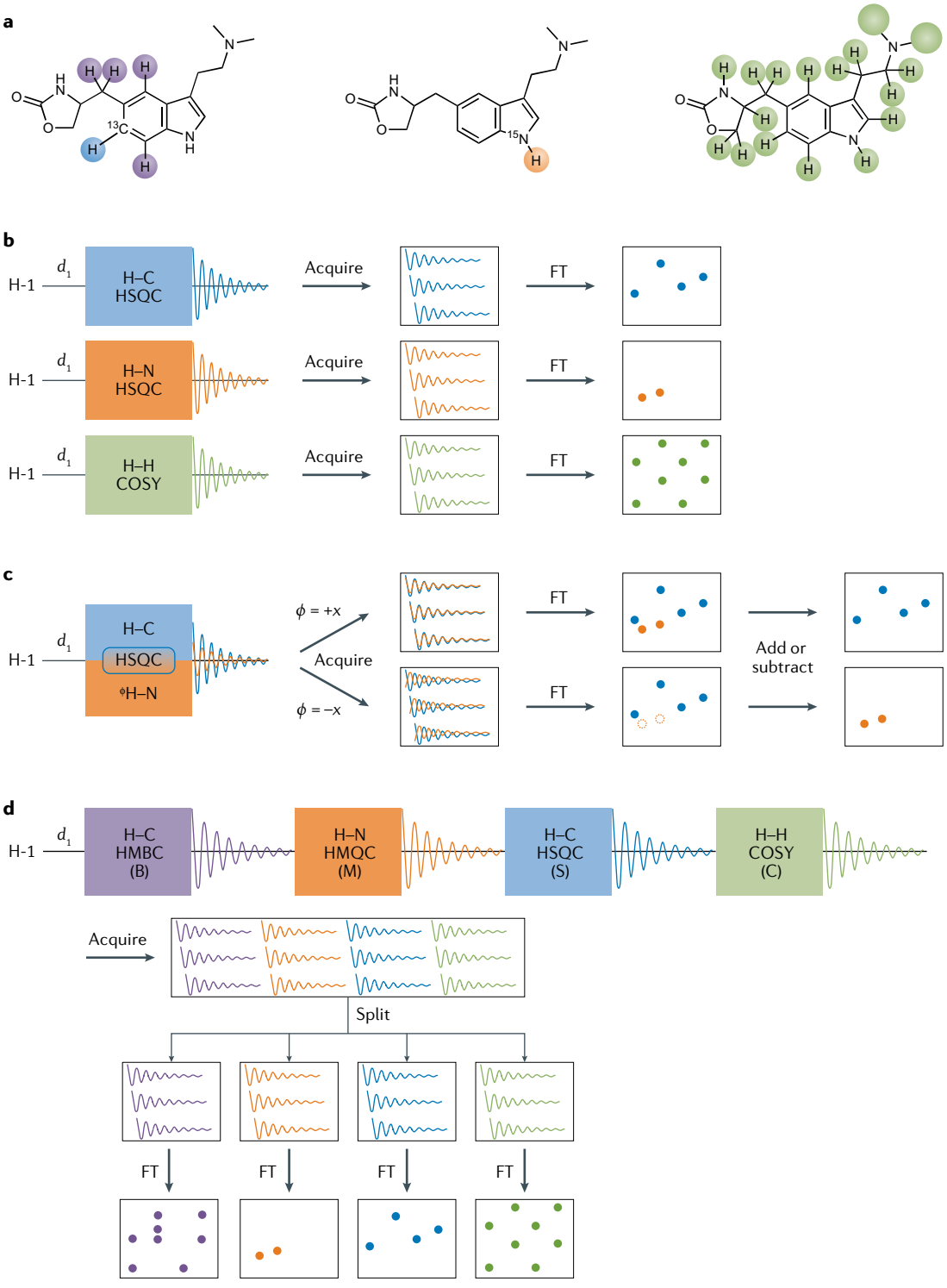

magnetization pools are consecutively sampled without intervening relaxation delays. NOAH supersequences are constructed by direct concatenation of suitably tailored modules that sample only their respective magnetization pools[16,53,54,57–59] (FIG. 4d), with each module designed to return other magnetization pools to equilibrium (+*z*). In these experiments, the FIDs are acquired independently and are initially stored in a file partitioned into multiple memory blocks. These blocks may be separated such that each experiment has its own matrix of raw data, after which processing takes place as usual. These procedures, which can generate multiple data sets from one experiment (up to five in the case of NOAH to date[16]), are typically invisible to the end user as they are executed by automated processing scripts. These scripts also make it possible to run these experiments under automation, which is essential for optimizing throughput.

An alternative strategy for sequential acquisition is polarization sharing, where a magnetization pool is divided into multiple portions that are independently manipulated and detected. This is most readily achieved by the preservation of equivalent pathways scheme[60] employed, for example, in HSQC[61] and TOCSY[62] experiments, where following t_1 evolution there are orthogonal (that is, cosine-modulated and sine-modulated) components that can be separately manipulated[63–65]. In a TOCSY experiment, these components can be subjected to different durations of isotropic mixing, thereby yielding two TOCSY spectra from one experiment displaying a different set of correlations[63]. Likewise, the two HSQC pathways can be used to separately generate HSQC spectra with different F_1 spectral widths[65], both coupled and decoupled HSQCs, or HSQC and HSQC–TOCSY spectra from the respective components[63]. Alternatively, pulse sequence elements such as BANGO can be used to excite only a portion of magnetization for one module[51,52], retaining the remainder for use in a subsequent module[66]. It should be noted that all such polarization sharing methods suffer from decreased sensitivity. Nonetheless, the time savings still represent a substantial benefit for samples that are not sensitivity-limited.

Lastly, a magnetization pool can also be sequentially sampled by subjecting magnetization that has already been detected once to another mixing process before sampling it again. For example, the HMBC experiment ordinarily records correlations between ^{13}C and ^{1}H nuclei separated by two or three bonds. Appending a COSY mixing period after the HMBC acquisition transfers magnetization from ^{1}H nuclei to other ^{1}H spins coupled to them; this yields an HMBC–COSY spectrum where ^{13}C nuclei are correlated with precisely those coupled partners, which are typically three or four bonds away from the original ^{13}C nuclei. Applying such mixing periods more than once opens up novel possibilities such as HMQC–COSY or HMBC–COSY relay chains for stepwise detection of through-bond correlations[67]. Such strategies can be further combined with time-sharing principles to create even more information-rich experiments[15].

All of these parallelized experiments share one major feature in common: they enable the collection of multiple 2D spectra with a single recovery delay (compare FIG. 4b–d), thus providing significant reductions in the time needed to obtain all of the constituent spectra. Furthermore, as long as *S*/*N* in the parallelized sequence is not excessively compromised, these time savings can also be translated into an overall gain in sensitivity per unit time, as they allow more transients to be collected in the same duration.

Multinuclear detection experiments

Basic multinuclear detection techniques. Typical NMR systems are designed with multinuclear functionality in mind. For instance, most commercial probes are built to allow simultaneous irradiation and detection of up to five nuclei. However, until recently, commercial NMR consoles were equipped with only a single receiver and, for sensitivity reasons, most NMR experiments were designed to involve ^{1}H detection. However, direct detection of hetero nuclei (X) has important advantages such as better resolution[68] and advantageous relaxation properties[69]. Furthermore, cryogenic high-temperature superconductor probes optimized for direct detection of hetero nuclei can potentially increase the sensitivity of X-detected experiments by a factor of more than ten[70,71]. Together with the advent of commercial multiple receiver NMR systems, this has prompted the development and routine use of multinuclear detected experiments.

Three basic types of multinuclear data acquisition techniques are shown in FIG. 5a–c, parallel, interleaved and sequential acquisitions, each with their own pulse schemes. The parallel acquisition pulse schemes or PANSY[13] typically involve polarization transfer from more sensitive nuclei (usually ^{1}H) to less sensitive nuclei (^{13}C, ^{15}N, ^{19}F, ^{31}P and similar). In the conventional COSY experiment, one of the two orthogonal components of magnetization is discarded[72]; however, in the PANSY–COSY pulse scheme, it is transferred to other nuclear species for detection, which increases the amount of observed magnetization. Mutual decoupling of two nuclear species during parallel acquisition is not feasible and the PANSY technique is mainly applicable in situations where such decoupling is not essential, for instance if the mutual scalar couplings are unresolved and can be neglected. The repetition rate of the PANSY experiments is determined by the recovery time of the high γ nuclei that typically serve as the polarization source and usually have the shortest recovery time. However, this is not always the case. For instance, despite lower γ, the ^{19}F nuclei often have shorter recovery times than ^{1}H nuclei due to more efficient relaxation mechanisms[73].

Parallel acquisition experiments may not involve polarization transfer at all, for example if there is no scalar coupling between nuclear species of interest or in parallel relaxation measurements, diffusion measurements and similar pulse schemes with no polarization transfer between the nuclei of interest[14]. In such experiments, the repetition rate is determined by the slowest relaxing nuclear species.

The interleaved experiments (see FIG. 5b) are easy to design and are constructed simply by placing one of

Isotropic mixing
Transfer of *x*, *y* and *z* magnetization components (hence, isotropic) between *J*-coupled spin systems.

HMBC
(Heteronuclear multiple-bond correlation). An experiment that correlates an insensitive nucleus (such as ^{13}C or ^{15}N) with protons that are remote in a molecular structure (typically within two or three bonds) via their long-range scalar coupling.

PANSY
Parallel acquisition nuclear magnetic resonance spectroscopy.

Polarization
The degree of alignment of nuclear spins with the applied magnetic field that gives rise to an observable nuclear magnetic resonance signal.

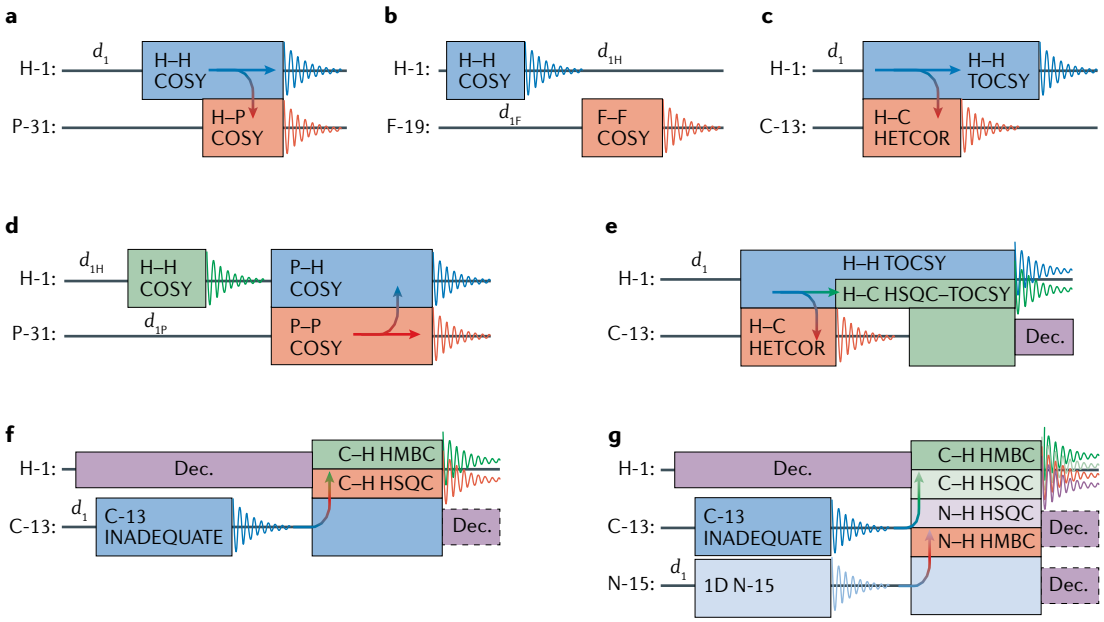

Fig. 5 | **Multinuclear acquisition techniques. a** | PANSY–COSY with parallel acquisition. **b** | Interleaved H–H COSY/F–F COSY. **c** | HETCOR/TOCSY with sequential acquisition. **d** | Interleaved COSY/PANSY–COSY. **e** | HETCOR/TOCSY/HSQC–TOCSY with sequential acquisition and time sharing. **f** | Basic PANACEA experiment. **g** | Extended PANACEA experiment. All experiments have a common recovery period (d_1), except for panels **b** and **d** where nuclei-specific recovery periods are indicated. Each channel is equipped with a separate receiver. Overlapping free induction decays (FIDs) denote time-shared data acquisition. Arrows indicate polarization transfer with colour coding that corresponds to the target spectra. Dec., decoupling; H-1, C-13 and so on, different radiofrequency channels corresponding to the nuclei they detect.

the two (or more) experiments into the recovery delay of the other experiment[74,75] (see also FIG. 2b). In practice, the standard pulse programmes are simply concatenated with minor adjustments. As the interleaved pulse sequences are cyclic, it does not matter which of the experiments is executed first. In this way, both recovery periods are used to record additional data. In practice, the total duration of the pulse sequence (τ_{pp}) and the data acquisition period (τ_{aq}) for 2D experiments is considerably shorter (approximately 100 ms) than a typical recovery period (d_1) (>1 s). If the recovery periods of the two nuclear species are very different, it may be possible to improve the efficiency of the interleaved experiments by placing several experiments involving fast relaxing nuclei in the recovery delay of slow relaxing nuclei[14]. Any disturbance of spins that are recovering must be avoided in order to preserve speed and sensitivity advantages.

For sequential detection experiments (see FIG. 5c), the pulse schemes involving sequential acquisition usually begin with transfer of otherwise unused magnetization from the more sensitive nuclei to the less sensitive nuclear species of interest. In addition to enhancing sensitivity, this often also reduces the experiment repetition rate determined by the typically shorter recovery times of the sensitive high γ nuclei. In these pulse schemes, one of the spectra is acquired during a long evolution period within the specially designed pulse sequence. Following the first acquisition period, the second part of the experiment is then completed and the second FID is acquired. For example, the 2D H–C HETCOR spectrum can be recorded during the mixing period of the 2D H–H TOCSY experiment[13]. In this experiment, the isotropic H–H mixing sequence of the TOCSY pulse scheme works as a composite pulse decoupling for the HETCOR scheme to produce a fully decoupled HETCOR spectrum (see FIG. 5c). Once the HETCOR data are acquired, the final part of the TOCSY experiment is executed. Similar techniques have been employed in biomolecular NMR, where magnetization of one of the experiments is stored on slowly relaxing nuclei (for example, ^{15}N) during the acquisition period of an alternative experiment[76,77].

Combining techniques with direct multinuclear detection. Experiments involving direct detection of multiple FIDs may combine several basic techniques. For example, the COSY/PANSY–COSY scheme shown in FIG. 5d combines parallel and interleaved acquisition methods. This experiment records three 2D spectra (H–H COSY, P–P COSY and P–H COSY) in the time of one conventional 2D COSY experiment. Likewise, experiments of different dimensionality can be combined using the techniques discussed above. For example, the 2D HETCOR/TOCSY pulse scheme has been modified to allow the recording of a 1D ^{13}C spectrum of non-protonated carbons in parallel with 2D H–C HETCOR using the time-shared acquisition technique[78]. Similarly, the sequential 2D HETCOR/TOCSY experiment has been extended to acquire 2D H–H TOCSY and 3D H–C HSQC–TOCSY spectra in a time-shared manner[79,80] (FIG. 5e). In FIG. 5e, a polarization sharing scheme is used to split the ^{1}H–^{13}C magnetization between the HETCOR and HSQC–TOCSY pulse

HETCOR
(Heteronuclear correlation). A technique for correlating an insensitive nucleus (such as ^{13}C) with neighbouring proton(s) via scalar coupling while using direct detection of the insensitive nucleus.

schemes, sacrificing some of the sensitivity advantage. Projection spectroscopy is employed to acquire tilted 2D projections of the 3D HSQC–TOCSY experiment and significantly reduces the experiment time[81,82].

The PANACEA experiment combines 2D ^{13}C-detected INADEQUATE with ^{1}H-detected 2D HSQC and 2D or 3D *J*-HMBC into a single supersequence[83]. A block diagram of the basic PANACEA pulse scheme based on sequential acquisition of ^{13}C- and ^{1}H-detected spectra is shown in FIG. 5f. The PANACEA supersequence is built around the 2D C–C INADEQUATE pulse scheme, which provides one-bond C–C connectivities[84,85]. Although the 2D INADEQUATE experiment is the least sensitive in the PANACEA supersequence because it is designed to detect pairs of directly bound ^{13}C nuclei with naturally low abundance (approximately 0.012%), it is one of the most powerful tools for structure elucidation of small organic molecules as it traces down the skeleton of organic molecules. Usually, 99% of the bulk ^{13}C magnetization from molecules containing a single ^{13}C isotope is destroyed in the conventional INADEQUATE pulse schemes. In the PANACEA experiment, however, this magnetization is recorded in a time-shared manner to produce a 1D ^{13}C spectrum and then further used in a 2D ^{13}C–^{1}H HSQC experiment acquired sequentially that exploits the high sensitivity of ^{1}H detection. Owing to the low sensitivity of the INADEQUATE scheme, highly concentrated samples are needed. Consequently, the HSQC experiment can be recorded with very few scans. Once the HSQC spectrum is acquired, the ^{13}C decoupling is switched off and the HSQC pulse scheme is replaced with the HMBC sequence. The INADEQUATE spectrum typically requires a significant (often >64) number of scans. This can be exploited to record up to three HSQC spectra separating CH, CH_2 and CH_3 resonances. Several HMBC spectra may be recorded to cover a rather large spread of the long-range ^{1}H–^{13}C couplings. Alternatively, a 3D C–H *J*-HMBC spectrum is acquired. Thus, the sensitivities of individual experiments are balanced by adjusting their acquisition times — less time is used to record the more sensitive spectra. Consequently, in a single measurement, the basic PANACEA experiment delivers 1D ^{13}C, 2D C–C INADEQUATE, three multiplicity edited 2D H–C HSQC spectra and several 2D H–C HMBC spectra or a 3D *J*-HMBC spectrum.

The 1D ^{13}C spectrum can also be used to eliminate spectral distortions caused by environmental instabilities, such as temperature variations and magnetic field fluctuations. This allows recording of the PANACEA spectra in pure liquids and eliminates the need for deuterated solvents[71]. In concentrated samples, such as cholesterol (1 M in $CDCl_3$), the basic PANACEA can be recorded in as little as 20 min. Sensitivity permitting, the experiment duration can be further reduced to just 56 s by exploiting Hadamard encoding[86]. Together with Hadamard encoding, spectral aliasing[87] has also been used to further reduce the measurement time. The extended version of the PANACEA experiment (FIG. 5g) involves recording of a 1D ^{15}N spectrum in parallel with the ^{13}C INADEQUATE followed by time-shared acquisition of the ^{15}N HSQC and HMBC spectra in parallel with the corresponding ^{13}C spectra, delivering 11 spectra in a single measurement.

The PANACEA experiment has been modified to replace the ^{13}C-based pulse schemes with their ^{29}Si analogues for studies of silicon oils[88]. As there are no Si–H bonds in silicone oils, the HMBC module is discarded and the HSQC module is optimized for long-range ^{1}H–^{29}Si couplings.

Results

The most significant use of 2D NMR spectra remains the structural verification and elucidation of small molecules via heteronuclear and homonuclear correlation experiments, such as those summarized in BOX 1. Accelerated data acquisition and the recording of multiple experiments offered by parallel NMR techniques enable a rapid identification of spin correlations within a molecular structure (yielding connectivity) and spatial proximity between nuclei (defining stereochemistry) following conventional data analyses procedures[89,90].

Parallel NMR with multiple microcoils

The electronic set-up shown in FIG. 2 has been used with an eight-coil probe head to acquire high-resolution 2D proton spectra from small molecules. Automatic shimming on the central two coils was used as a starting point, and then manual shimming used for fine adjustment to determine a 'universal shim setting' that produces linewidths in the low-hertz range for each of the samples. With careful construction, the 90° pulse durations for each coil were essentially identical.

COSY, TOCSY and gradient COSY spectra from sucrose, galactose, arginine, chloroquine, cysteine, caffeine, fructose and glycine samples, one of each in each coil, are shown in Supplementary Table 1. As long as the data from each coil are stored separately, then standard data processing can be applied; that is, zero-filling, filtered with an appropriate window function, symmetrized and displayed in either magnitude or phase mode[72,89].

Homonuclear multi-FID detection

Advantages of multi-FID detection. The duration of a typical NMR sequence T_{exp} is generally given by:

$$T_{exp} = N(d_1 + \tau_{pp} + \tau_{aq}) \quad (4)$$

where τ_{pp} is the duration of the pulse programme, τ_{aq} is the data acquisition (FID) time, d_1 is the recovery delay and N is the total number of scans. In *n*D experiments, the pulse sequence duration τ_{pp} is typically a few milliseconds and, usually, is the shortest of the three components of Eq. 4, except in NOESY, ROESY or TOCSY experiments with long mixing periods. The acquisition time τ_{aq} is the next-shortest component (approximately 100 ms), and the recovery delay d_1 is the longest pulse sequence element (typically 1–5 s).

In parallel NMR spectroscopy that incorporates M conventional experiments, the time savings provided by multi-FID experiments are defined by the ratio ρ_t:

$$\rho_t = \frac{\sum_{i=1}^{M} T_{exp}(i)}{T_{exp}(\mathrm{MF})} = \frac{\sum_{i=1}^{M} [d_1(i) + \tau_{pp}(i) + \tau_{aq}(i)]}{T_{exp}(\mathrm{MF})} \quad (5)$$

PANACEA
(Parallel acquisition nuclear magnetic resonance). An all-in-one combination of experimental applications: a method that combines three standard pulse sequences (INADEQUATE, HSQC and HMBC) into a single supersequence.

INADEQUATE
(Incredible natural abundance double-quantum transfer experiment). A method for correlating adjacent insensitive nuclei (typically ^{13}C) via one-bond scalar coupling.

Linewidths
Widths of nuclear magnetic resonance peaks at half height, usually defined in hertz.

NOESY
(Nuclear Overhauser effect spectroscopy). A technique for identifying nuclei, most often protons, that are close in space (typically <5 Å) and, hence, share dipolar coupling.

ROESY
(Rotating-frame Overhauser effect spectroscopy). A technique related to NOESY that is also used to identify spatial proximity between protons.

where $T_{exp}(i)$ is the duration of the ith conventional experiment, and T_{exp}(MF) is the duration of the multi-FID experiment. As the speed-up arises from the elimination of recovery delays, the value of ρ_t depends on how significant these delays are as a proportion of total experimental time. In the limit where τ_{pp} and τ_{aq} are negligible compared with d_1, ρ_t will be equal to M, the number of experiments combined into (or number of FIDs acquired in) one sequence.

Parallel NMR spectra provide identical information to those obtained from conventional measurements, but in a reduced time frame as reflected in ρ_t. Given all other parameters in Eq. 1 are equal, the performance of the parallelized experiments can be measured in terms of the relative sensitivity enhancement per unit time ε_t for each module, as defined by:

$$\varepsilon_t = R_S \rho_t^{1/2} \quad (6)$$

where R_S is a factor indicating the sensitivity losses due to parallelization; that is, the relative signal intensity from the parallelized experiment with respect to an equivalent conventional experiment acquired with the same parameters.

Practical examples. Time-shared experiments that detect two different signals have a maximum attainable ε_t value of $2^{1/2} \approx 1.41$. In practice, slightly lower sensitivity improvements are observed due to necessary compromises in delay timings, which result in a reduced R_S factor. For example, the careful optimization of a time-shared sensitivity-enhanced HSQC yielded ^{15}N and ^{13}C ε_t improvements of 1.34 and 1.07, respectively, for doubly labelled proteins[91]. Likewise, time-shared HSQC–TOCSY experiments provided ^{15}N and ^{13}C ε_t improvements of 1.36 and 1.21, respectively, for natural abundance samples[92].

For NOAH supersequences using sequential acquisition, up to five experiments have been combined[16], yielding concomitant increases in ρ_t. A selection of NOAH experiments are presented in TABLE 2, along with their values of ρ_t and ε_t. As all modules in a supersequence share the same recovery delay d_1, the incorporation of additional modules leads to minimal increases in experiment time, which arise only from τ_{pp} and τ_{aq} of the newly added module(s). In general, the gains in sensitivity per unit time ε_t in the NOAH experiments increase with the number of modules M as exemplified in TABLE 2, rows 1–3. The exact value of ρ_t depends on the relative sizes of τ_{pp}, τ_{aq} and d_1.

Supersequences involving NOESY modules will typically have ρ_t somewhat smaller than the number of modules M, because of the relatively long mixing time (500 ms in these examples) that contributes to τ_{pp}. For example, the NOAH-2 MS supersequence has a ρ_t of 1.90, which is closer to 2 than the SN supersequence (TABLE 2, rows 1 and 4). However, COSY experiments can be fully nested within the NOESY pulse sequence using the COCONOSY scheme[93,94], which means that an extra module can be recorded without any increase in experimental time (compare rows 1 and 2 in TABLE 2). The NOAH-4 MSCN spectra of cyclosporine and the relative sensitivity advantages ε_t across the NOAH experiments (TABLE 2, rows 1–3) are illustrated in Supplementary Fig. 3. The threefold reduction of experimental time ($\rho_t = 3.01$) leads to significant sensitivity enhancements per unit time.

As mentioned above, the primary benefit arising from parallelization is accelerated data collection, with increases in sensitivity per unit time relative to conventional data collection a secondary gain in some instances. To what extent such gains are realized depends strongly on the supersequence employed, molecular properties (nuclear relaxation times), sample conditions (solvent properties, temperature) and experimental parameters (recovery delays and acquisition times). The gains indicated in TABLE 2 should therefore be viewed as representative values typical for the characterization of small organic molecules.

Table 2 | **Sensitivity and speed advantages by NOAH supersequences**

Entry	NOAH[a]	M	T_{exp}(MF)	$\Sigma_i^M T_{exp}(i)$	Speed ρ_t	Sensitivity advantage ε_t
1	SN	2	19 min 38 s	33 min 16 s	1.69	1.30 (S), 1.30 (N)
2	SCN	3	19 min 38 s	47 min 38 s	2.42	1.56 (S), 1.39 (C), 1.50 (N)
3[b]	MSCN	4	20 min 39 s	62 min 5 s	3.01	1.73 (M), 1.50 (S), 1.38 (C), 1.61 (N)
4	MS	2	15 min 11 s	28 min 54 s	1.90	1.38 (M), 1.20 (S)

The sample was cyclosporin (50 mM in C6D6). Two scans were acquired for each increment, with 256 t_1 increments per module. A recovery delay (d_1) of 1.5 s was used for all experiments. T_{exp}, experiment time; T_{exp}(MF), duration of multi-free induction decay experiment; t_1 is the time period associated with the indirectly encoded frequency dimension. [a]Single-letter codes for NOAH modules: M, ^{1}H–^{15}N HMQC; S, ^{1}H–^{13}C HSQC; C, ^{1}H–^{1}H COSY; N, ^{1}H–^{1}H NOESY (mixing time of 500 ms). [b]See Supplementary Fig. 3.

Multinuclear detection schemes

Basic experiments. Three typical examples of parallel, interleaved and sequential acquisition experiments with multinuclear detection involving abundant nuclei (^{1}H, ^{19}F and ^{31}P) and magnetically diluted nuclei (^{13}C) are shown in FIG. 6. One of the simplest and most versatile experiments is the COSY pulse scheme. The dual receiver 2D H–P PANSY–COSY experiment records homonuclear (H–H) COSY and heteronuclear (H–P) COSY spectra in the same experiment time as is normally required to acquire a single conventional 2D COSY spectrum (see FIG. 6a). Both spectra share the t_1 evolution period and therefore the F_1 (^{1}H) frequency axis, which ensures peak alignment in the two spectra and facilitates the resonance assignment in complex spectra.

An example of an interleaved H–H/F–F COSY experiment is shown in FIG. 6b. In this case, two homonuclear 2D COSY spectra are recorded in the same time it takes to record one conventional COSY experiment involving nuclei with the longest recovery time, in this case ^{1}H. Similar interleaved experiments can involve more complex pulse schemes[14], other abundant nuclei (for example, ^{31}P)[54] or isotopically enriched samples[95,96].

Spectra recorded using a 2D H–C HETCOR/H–H TOCSY pulse scheme that employs sequential acquisition are shown in FIG. 6c. In this example, diluted nuclear species (^{13}C) have been chosen. Generally, the HETCOR spectra contain the same information as the corresponding HSQC spectra, but can be recorded

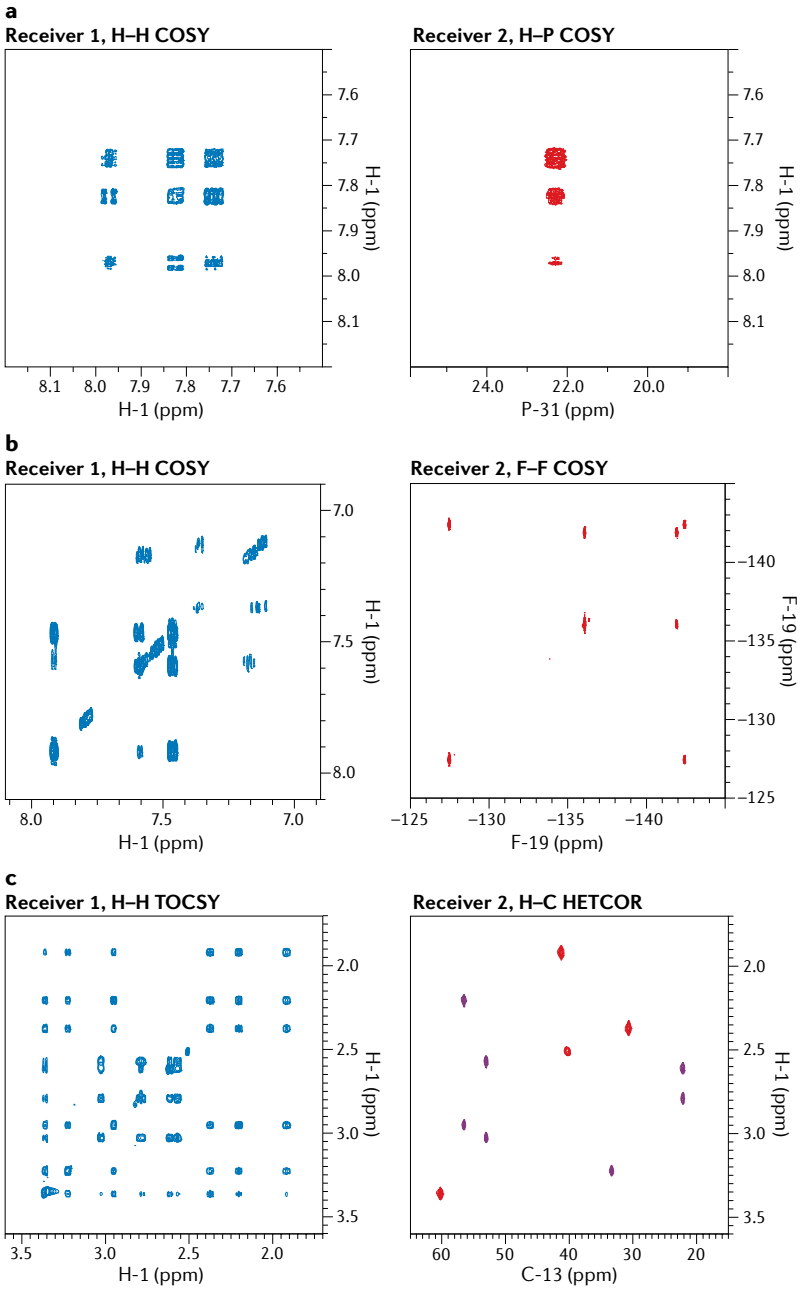

Fig. 6 | **Spectra recorded with basic dual-receiver pulse schemes. a** | H–H/H–P COSY spectra of $P(Ph_4)^+Cl^-$ recorded with parallel acquisition (see FIG. 5a). **b** | H–H/F–F COSY spectra of a mixture of 2,4,5-trifluorobenzoic acid and 2,3,6-trifluorobenzoic acid recorded with an interleaved experiment (see FIG. 5b). **c** | C–H HETCOR/H–H TOCSY of gibberellic acid recorded with a sequential acquisition experiment (see FIG. 5c). Note the joint F_1 frequency axis in panels **a** and **c** that guarantees perfect peak alignment in the complementary spectra.

faster and with better resolution. However, this requires relatively high sample concentrations (>20 mM) owing to the low ^{13}C sensitivity and low natural abundance (1.1%), and there is no sensitivity advantage in this particular case.

Combined multinuclear detection schemes. Various combinations of the basic parallelization techniques have yielded sophisticated, efficient and information-rich experiments. For instance, interleaved H–H COSY and P–P/P–H PANSY–COSY spectra recorded using the pulse scheme of FIG. 5d are shown in FIG. 7. The three 2D spectra were recorded in the time that is required to acquire a single conventional 2D H–H COSY spectrum, not only providing correlations within but also between the homonuclear ^1H and ^{31}P spin systems. In addition to saving time ($\rho_t = 3$), this experiment detects more magnetization per unit time, offering considerable sensitivity improvements ($\varepsilon_t = 1.73$). Similarly, a supersequence that combines the PANSY–COSY module (C^2) with the NOAH technique BSCC[2] can record five spectra in a single measurement (H–C HMBC, H–C HSQC, H–H COSY, P–P COSY and P–H COSY)[54]. The C^2 module can easily be appended to many other NOAH supersequences. An example of spectra recorded using the NOAH-4 SCRC[2] supersequence is shown in Supplementary Fig. 4.

The HETCOR/TOCSY/HSQC–TOCSY experiment[79,80] (see FIG. 5e) effectively delivers 3D information in the time of a 2D experiment by simultaneously recording two orthogonal 2D projections — the HETCOR and TOCSY spectra — together with tilted projections of the 3D multiplicity edited HSQC–TOCSY[81,82]. The increased dimensionality in combination with C–H multiplicity editing and non-uniform sampling provided highly resolved spectra, significantly reducing spectral overlap and the related resonance assignment ambiguities.

The PANACEA spectra of quinine recorded using the pulse scheme of FIG. 5f are shown in FIG. 8, which also details small-molecule structure elucidation steps from these spectra[83]. First, the number of carbon atoms is obtained from the 1D ^{13}C spectrum (FIG. 8a). The INADEQUATE spectrum reveals how the carbon atoms are interconnected (FIG. 8b, dotted lines), tracing down the carbon skeleton of the molecule (FIG. 8c). The multiplicity edited HSQC spectra (FIG. 8d) reveal the number of hydrogen atoms attached to each carbon site (FIG. 8e). Finally, the HMBC spectra (FIG. 8f) connect molecular fragments separated by heteroatoms (FIG. 8g). The chemical shift information coupled with elemental analysis data reveals the final structure of the molecule (FIG. 8h).

The internal lock (or frequency correction) built into the PANACEA experiment allowed recording of spectra in pure peanut oil and neat silicon oil with no deuterium lock and no temperature regulation[71]. This highlights one of the main advantages of parallel NMR — all spectra are recorded under equivalent environmental and magnetic instabilities that can be corrected by post-processing. The latter involves measuring the frequency shifts in PANACEA 1D ^{13}C spectra and applying the correction to all other PANACEA spectra scaled according to their resonance frequencies. The highly accurate stereospecific long-range ^1H–^{13}C coupling information recorded in a high-resolution PANACEA experiment indicated the presence of an intramolecular hydrogen bond[97]. The extended PANACEA pulse scheme of FIG. 5g applied to a nitrogen-containing organic molecule (melatonin) yielded 1D ^{15}N, 2D N–H HSQC and 2D N–H HMBC spectra in addition to the basic PANACEA data[83], thus facilitating structure elucidation.

Parallel ultra-fast NMR

Single-scan 2D NMR can be combined with other techniques. One such combination involves nuclear hyperpolarization, as has been demonstrated in the realm of natural products[98]. The 2D single-scan C–H HMBC and HSQC spectra of limonene, α-pinene and camphene (1:1:2 mM) solution were acquired sequentially in a single measurement lasting only a few hundred milliseconds. The 4.4 µl sample was polarized with microwaves at 1.4 K in a Hypersense (Oxford Instruments) polarizer and then dissolved in warm methanol-d_4 before being transferred to a 500-MHz Varian Inova NMR spectrometer. The spectral aliasing combined with selective excitation was used to reduce the 150 ppm ^{13}C observation bandwidth and to preserve non-protonated ^{13}C magnetization prior to the single-scan HSQC pulse scheme for use in the sequential HMBC experiment.

Ultra-fast 2D NMR can also be combined with parallel techniques of multi-FID detection discussed in the previous sections. For instance, combining the ultra-fast COSY methodology with the parallel acquisition COSY experiment (see FIG. 5a) enables recording of several *n*D spectra in a single scan[99]. The methodology is accordingly named PUFSY (parallel ultra-fast spectroscopy).

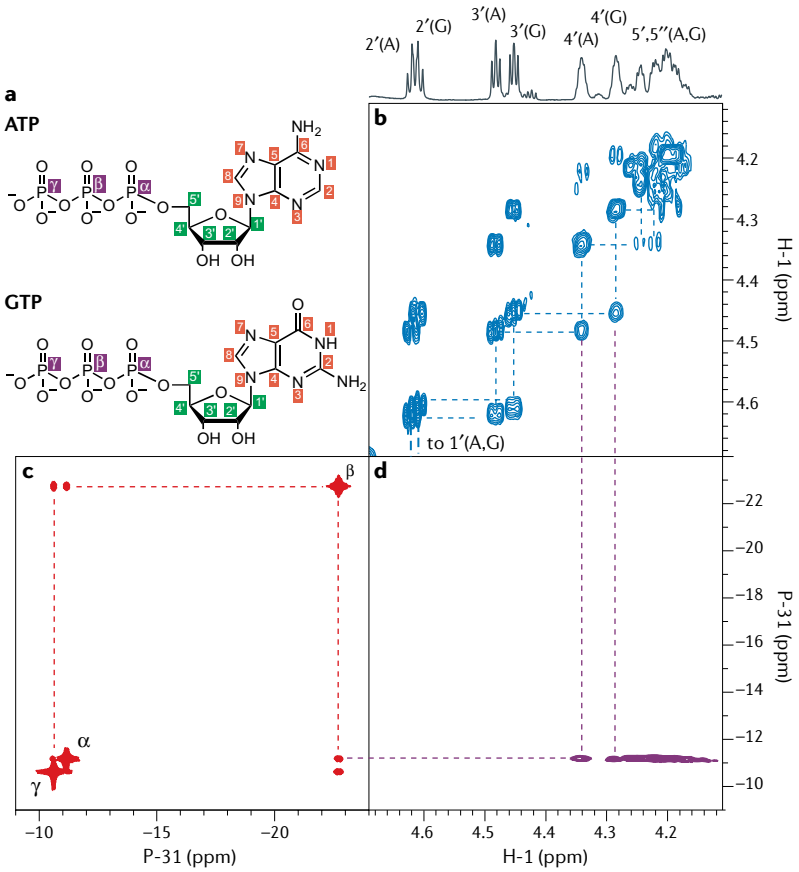

Fig. 7 | **Interleaved H–H COSY and P–P/P–H PANSY–COSY spectra of a mixture of ATP and GTP in D_2O. a** | Structure of ATP and GTP. Top trace shows peak assignment in the one-dimensional (1D) proton spectrum. **b**–**d** | Connectivity of resonances (dotted lines) in H–H COSY spectrum (blue, panel **b**), P–P COSY spectrum (red, panel **c**) and H–P COSY spectrum (pink, panel **d**) linking the ^{1}H and ^{31}P spin systems in parts **b** and **c**. Spectra recorded on a 700-MHz (^{1}H) Bruker NEO spectrometer equipped with the QCIP cryoprobe. Experiment time 10 min.

Two examples of H–H/H–F PUFSY–COSY spectra of fluorinated compounds recorded on a spectrometer equipped with two receivers are shown in FIG. 9. Each pair of the 2D PUFSY spectra was recorded in about 100 ms. The 2D H–H and H–F COSY spectra recorded in parallel were stored in separate memory locations, each processed and analysed as individual ultra-fast spectra (see FIG. 3b). Computer-optimized folding was used to reduce the large ^{19}F spectral window and the associated gradient amplitudes. Similar experiments involving ^{31}P were also reported[99]. These experiments serve as a proof of principle with potential applications in studies of fast chemical reactions, in biochemical interactions and in hyperpolarized samples.

Applications

In this section, we discuss various applications of parallel NMR techniques. In addition to more efficient NMR spectra acquisition, each of these techniques offers unique ways of obtaining new information. Probes equipped with multiple microcoils allow simultaneous monitoring of multiple samples offering new insights into electrophoretic separations and diagnostic NMR. Ultra-fast NMR methodology finds applications in real-time monitoring of chemical reactions and biophysical rearrangements. Multi-FID detection techniques involving one or more receivers elucidate small-molecule structures from a single measurement.

Multiple microcoils

Multiple microcoils enable the time efficiency of studies of mass-limited samples to be increased significantly, up to a factor equal to the number of coils. However, they also enable information to be more easily acquired because of the multiple coils. For example, Raftery and colleagues devised a difference probe[26], in which the degree of cancellation of common signals from each probe was 90%, that enabled identification of protein–ligand interactions using glutathione and glutathione *S*-transferase binding protein. Ciobanu et al. described how multiple microcoils can be used to increase the temporal sampling frequency of chemical reactions induced in small sample volumes via micromixers[35]. Wolters et al. demonstrated that a dual probe could be used in interleaved mode to overcome some of the disadvantages of coupling electrophoretic separations with microcoil NMR detection[34]. There have also been applications of multiple microcoils in microscopic MRI[100] as well as diagnostic magnetic resonance[101].

FIGURE 10 shows a photograph of a dual-coil, multi-frequency, probe head that can be used for protein samples. The small solenoidal coils have an active volume of 15–20 µl, requiring only small quantities of isotopically labelled protein. Each of the two coils were tuned to both ^{1}H and ^{15}N frequencies, and a single external lock coil was also integrated. The high spectral quality achievable using this probe is highlighted in FIG. 10, where one coil was loaded with 1.25 mM ^{15}N-labelled ubiquitin (highly structured; FIG. 10b) and the other contained a sample of 1 mM ^{15}N-labelled yeast proteinase A inhibitor (IA-3) (intrinsically unstructured; FIG. 10b) in low-deuterated buffer solutions.

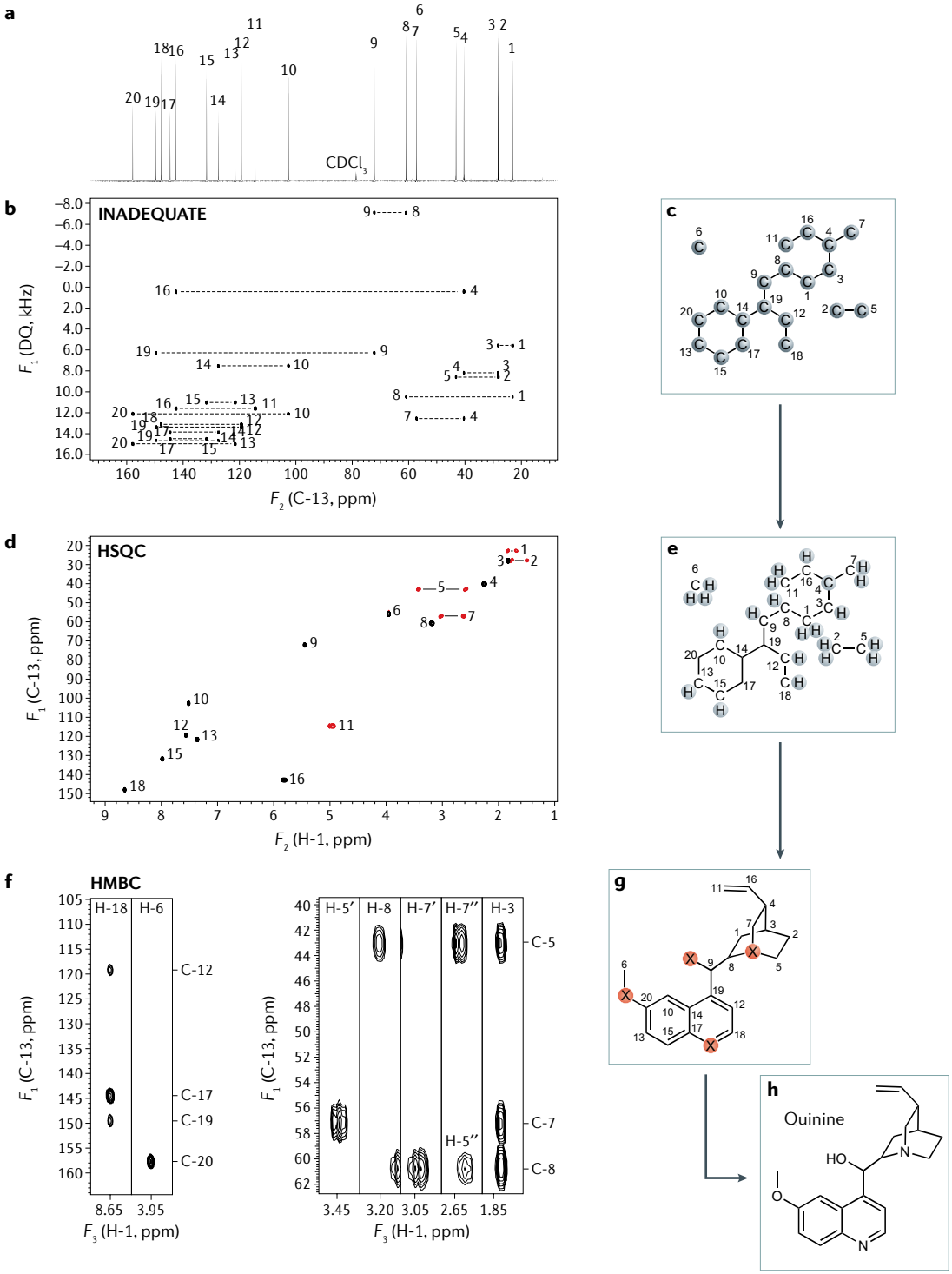

Applications of single-scan nD NMR

Spatio-temporal encoding can provide the ultimate parallelization, but it does so at the price of reduced sensitivity. When considering potential applications, the question thus arises of when such a price is worth paying. One family of experiments where spatio-temporal encoding proves useful is in case of time-dependent samples, where either the compounds' lifetimes are incompatible with conventional *n*D acquisitions or time instabilities become the dominant sources of noise — particularly of t_1 noise. Applications include homonuclear and heteronuclear acquisitions on unstable magnets[102], monitoring of organic reactions as they happen[103–106] and real-time monitoring of biophysical rearrangements on proteins and nucleic acids[107,108] (see FIG. 11). Furthermore, the single-shot homonuclear 2D ^{1}H correlations are also well suited for monitoring the flow of metabolites and chemicals — for instance, as they elute out from a chromatographic column and through an NMR spectrometer acting as a detector[109,110].

As mentioned, a particularly intriguing combination arises from merging high-speed and limited sensitivity

◀ Fig. 8 | **Step-by-step manual structure elucidation from the PANACEA spectra.** **a** | A one-dimensional (1D) ^{13}C spectrum indicating the number of carbon atoms. **b**,**c** | 2D INADEQUATE spectrum (panel **b**) provides C–C connectivities (dotted lines). This traces down the carbon skeleton of the molecule (panel **c**). **d**,**e** | Multiplicity edited HSQC spectrum (panel **d**) revealing the number of attached protons (CH_2 signals are negative, shown in red) as shown in (panel **e**). **f**,**g** | HMBC spectra (panel **f**) connect the molecular fragments (panel **g**). **h** | Last step establishes nature and position of heteroatoms (X) as revealed by chemical shifts and elemental analysis. All spectra were recorded on a Varian NMR system equipped with a cryogenic high temperature superconductor (HTS) probe optimized for ^{13}C detection and operating at 500 MHz (^1H) in a single measurement using the basic PANACEA pulse scheme shown in FIG. 5f[83]. F_1, double quantum (DQ) frequency axis.

ultra-fast 2D NMR with nuclear hyperpolarization. These methods can have much greater signal intensities than conventional NMR samples, but limited measurement lifetimes. An early example of this was provided by the combination of homonuclear single-shot 2D NMR and CIDNP, an optical enhancement technique leading to photobleaching after a few scans[111]. Sensitivity and speed enhancements of approximately three orders of magnitude each were subsequently demonstrated by the combination of ex situ dynamic nuclear polarization and heteronuclear single-shot 2D NMR[98,112,113]. Homonuclear single-scan 2D correlations relying on enhancements derived from parahydrogen have also been implemented[114]. Single-scan 2D spectral–spatial correlations have also been demonstrated in this manner, including in hyperpolarized and thermal preclinical as well as clinical human MRI settings[115–119]. As mentioned, the spatial extent of a homogeneous sample can also be used to encode other sorts of information besides chemical shifts of evolving spins. The measurement of relaxation times[43] and of molecular self-diffusivities[44,45], for instance, has also been sped up in this manner. More recent applications of ultra-fast NMR can be found elsewhere[120–123].

Structure elucidation from a single supersequence

The PANACEA experiment. A step by step example of manual structure elucidation of quinine from the PANACEA spectra is shown in FIG. 8. Although computer-assisted structure elucidation can be used, it was not available at the time when the experiment was published. This example is used to demonstrate the power of the INADEQUATE experiment that makes the manual structure elucidation easy. The 1D ^{13}C spectrum of the quinine in $CDCl_3$ recorded in the PANACEA experiment (top panel) provides the number of carbon atoms in the molecule. The 2D INADEQUATE spectrum reveals the connections between the carbon atoms. Some connections are interrupted by heteroatoms leaving several fragments disconnected from the main scaffolding. The HSQC spectrum provides information about the number of protons attached to the corresponding carbon atoms and revealing potential sites for the missing heteroatoms. The HMBC spectra provide long-range correlations connecting the fragments and closing the rings. Finally, the nature of heteroatoms is revealed by the chemical shifts in combination with data from elemental analysis. Similar examples of structure elucidation based on the PANACEA experiment can be found elsewhere[71,83,88,97].

Although the structure elucidation based on the PANACEA spectra is simple and largely unambiguous, the main disadvantage of this experiment is the need for substantial amounts of sample. Cryoprobes optimized for direct ^{13}C detection can reduce the required sample amount by up to a factor of ten as compared with room-temperature probes[70,71]. ^1H-detected techniques coupled with CASE[90] (computer-assisted structure elucidation) and small-diameter cryoprobes have the potential to reduce the required sample amount even further, often to sub-milligram quantities.

CASE: from experiment direct to structure. BSC and BSCN-based NOAH supersequences (where the single-letter code B indicates HMBC, S indicates HSQC, C indicates COSY and N indicates NOESY) are capable of providing heteronuclear and homonuclear correlation information from a single experiment. Although this is possible with conventional sequences, the NOAH experiments achieve the same goal in a far shorter time and, for some combinations, with increased sensitivity. This not only enables optimal use of instrument time but should also prove to be critical for systems that are reacting or are otherwise unstable as it avoids temporal variations between individual experiments. The direct extraction of a molecular structure from NOAH spectra using CASE routines[90] (CMC-se) has been successfully demonstrated[53,54], and is illustrated here for the pharmaceutical zolmitriptan (FIG. 1 2). A single NOAH-4 BMSC experiment (M indicating ^{15}N HMQC) provided all necessary correlations for the structural identification and resonance assignment of the compound but required only one-third of the instrument time required by four conventional experiments of equal resolution ($\rho_t = 2.98$), illustrating the gains afforded through parallelization.

Although not the case for zolmitriptan, structure elucidation can occasionally be hampered by overlap in the proton dimension, which is particularly problematic in COSY spectra. In situations such as these, additional dispersion in a ^{13}C indirect dimension can prove highly useful, such as in 2BOB or H2OBC[124] experiments, which have been incorporated into multiple-FID sequences[54,125].

Applications in metabolomics

Metabolomics involves identification of metabolites — small molecules produced by cell metabolism in biological mixtures, such as bodily fluids (blood plasma, urine and so on) and tissue[70,126]. Parallelization of NMR methods potentially can increase sensitivity and throughput in metabolomics studies as well as mitigate the effects of sample degradation and environmental and instrumental instabilities that often complicate the analysis. To date, only one pulse scheme recording several spectra simultaneously, namely HETCOR/TOCSY/HSQC–TOCSY, has been applied to metabolomics studies designed with this specific application in mind[79,80]. One of the basic steps in analysis of NMR spectra of metabolomics samples is signal assignment, usually by 2D NMR techniques[70,126]. Although 3D NMR offers even higher resolution and is widely used in biomolecular studies, such techniques are deemed too time-consuming for

metabolomics applications to time-sensitive samples. Instead, the parallelized HETCOR/TOCSY/HSQC–TOCSY pulse scheme yields 3D information that is acquired in the time frame of a 2D measurement. The experiment achieved complete resonance assignment in a mixture of 17 amino acids and 4 common metabolites comprising a medium used in human in vitro fertilization[127], resulting in a reduction of the experiment time by an order of magnitude. This has opened new avenues for high-throughput metabolomics studies using NMR, even as similar combinations of multinuclear detection and projection spectroscopy have been used in biomolecular NMR[128,129]. Recent reports of ultra-fast NMR in metabolomics studies[130,131] are indicative of potential applications for parallel ultra-fast NMR methods in this field.

Reproducibility and data deposition

The spectra yielded by parallel acquisition techniques provide equivalent data to standard 2D experiments once the requisite processing has been undertaken. This means that spectral information may be reported in the same format as existing methods. For data reproducibility, it generally suffices to specify a subset of acquisition parameters that will have the greatest impact on spectrum appearance and quality. Precise details will vary according to the sequence in use but will most often include parameters that directly influence spectrum resolution, sensitivity and the transfer processes within the mixing period, such as spectral widths for each dimension and FID acquisition times, the recovery delay and number of transients, and experiment-specific parameters such as scalar coupling constants or durations of mixing periods. Significant instrumental details include the vendor, field strengths (expressed typically in terms of ^{1}H frequencies), detection probe characteristics (coil configurations and diameter) and sample temperatures. Where possible, the design of parallelized pulse sequences seeks to employ similar parameters to conventional experiments, standardizing nomenclature and, thus, simplifying their implementation. Similarly, as for conventional 2D data sets, parallelized data tend not to be suitable for quantitative measurements and attempts to use the experiments in this way would require suitable endeavours to establish their viability for such work.

For small organic molecules, metadata from processed spectra such as structural assignments, chemical shifts, coupling constants and integrals may also be stored in plain-text format according to the recent NMReDATA (extracted data) specification[132]. The file format

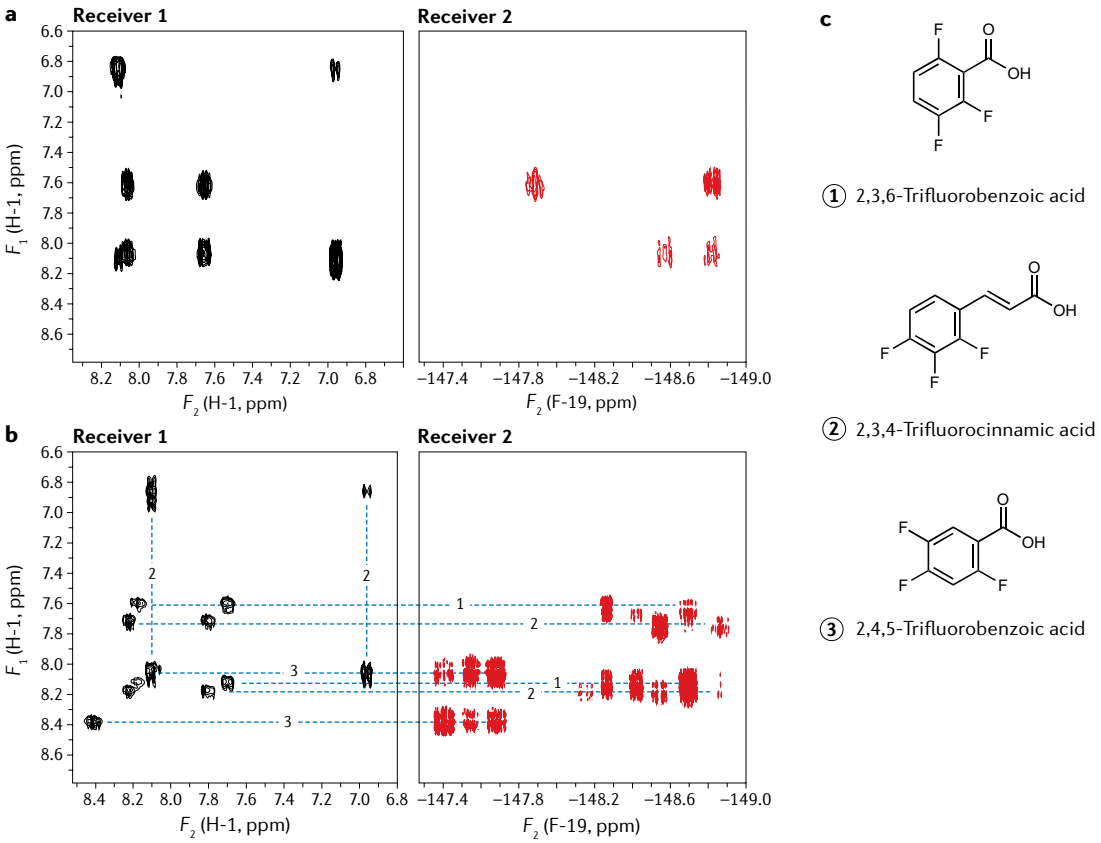

Fig. 9 | **Ultra-fast H–H and H–F PUFSY–COSY spectra recorded in parallel. a** | PUFSY (parallel ultra-fast spectroscopy) spectra of compound **2**. **b** | PUFSY spectra of a mixture of compounds **1**–**3**, all 5% solutions in DMSO-d_6. In both cases, the two spectra share the F_1 (^{1}H) frequency axis. Spectra recorded on a 600-MHz (^{1}H) Varian DDR spectrometer. Excitation and acquisition gradients $G_e = \pm 10$ G cm^{-1} and $G_{acq} = 14.9$ G cm^{-1}; acquisition time $T_{acq} = 488$ µs in 200 acquisition cycles (top spectra) and $T_{acq} = 490$ µs in 150 acquisition cycles (bottom spectra); a pair of 15-ms chirp pulses used for encoding the indirect dimension. Total experiment times 128 ms (top) and 104 ms (bottom). H-1, C-13 and so on, different radiofrequency channels corresponding to the nuclei they detect. Adapted with permission from REF.[99], Wiley.

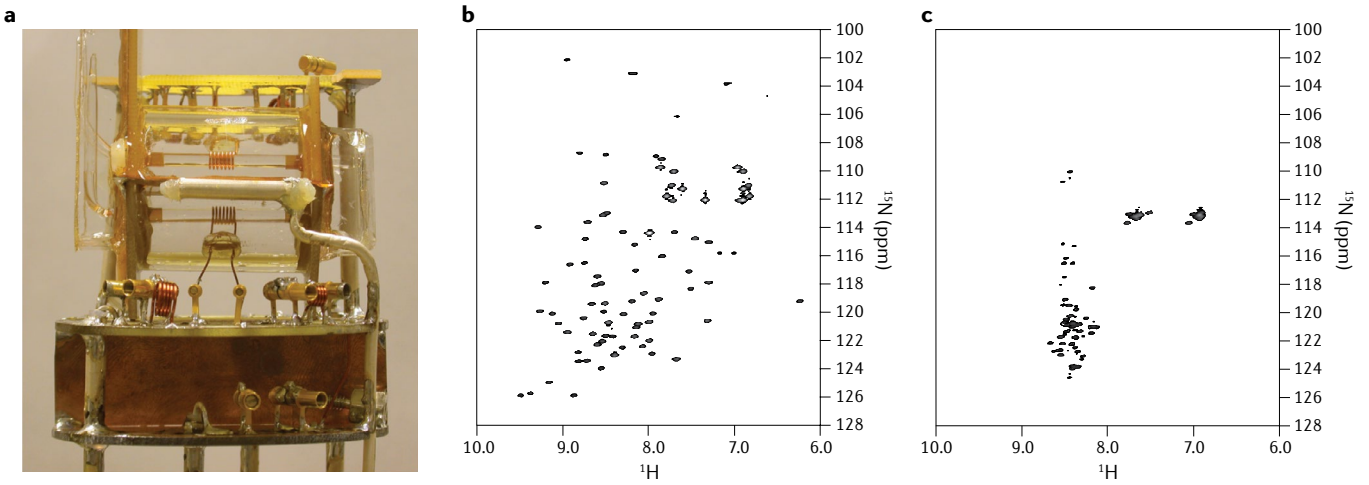

Fig. 10 | **Parallel studies of protein samples. a** | Photograph of the two-coil double-tuned probe with external lock coil and electronic circuitry. **b** | ^{1}H–^{15}N HSQC spectrum of 1.25 mM ^{15}N-labelled ubiquitin in H_2O/D_2O (9:1). Data matrix 1024 × 192 (states), 1 s water presaturation, 32 signal averages. Total data acquisition time 3.5 h. **c** | ^{1}H–^{15}N HSQC spectrum of 1 mM ^{15}N-labelled yeast proteinase A inhibitor (IA-3) in H_2O/D_2O (9:1), identical data acquisition parameters used. Interleaved data were acquired using a radiofrequency switch controlled from the pulse programme. Adapted with permission from REF.[161], Elsevier.

is an extension of the existing structure data format (SDF), which is compatible with the commonly used molfile format for describing molecular structures. The association of an NMReDATA file with the raw spectroscopic data from which it originates constitutes an NMR record. The NMR STAR (Self-defining Text Archival and Retrieval)[133–137] standard is particularly relevant for biomolecular NMR and includes the description of experiments, the data generated and the derived results such as molecular structures, dynamics and functional properties, whereas nmrML (markup language)[138] has been similarly promoted for metabolomics NMR data.

As with experimental parameters, new pulse programmes and any processing scripts should be made available to users in order to ensure reproducibility. Most often, these are included in the supplementary material sections of journal articles describing novel techniques and also through author websites. However, having a curated, centralized online 'library' of pulse programmes, such as the Bruker User Library, is a desirable alternative that is scalable, robust and more likely to be future proof. Ideally, instrument vendors may distribute these files together with NMR software releases; for example, numerous NOAH supersequences, as well as the associated scripts, are already distributed by instrument vendors.

Limitations and optimizations

NMR with multiple microcoils

The current limitations to the use of multiple microcoils are the number of coils that can fit into the bore of a standard NMR magnet and the number of receivers. Microfabrication techniques can potentially increase the number of coils, but as the sample volume becomes smaller so does *S*/*N*, leading to samples requiring higher concentrations. Commercial NMR systems are currently limited to four receivers, and the only way to increase the number of separate experiments is to time-domain multiplex the signals from more than four coils; there is no intrinsic limitation to the number of channels, so we anticipate that this may increase in the future. When considering sample preparation and handling, one of the biggest challenges is producing samples with microvolumes closely matched to that of the microcoil, and delivering the sample to the coil accurately and reproducibly. One possibility is to use microdrop technology or zero-dispersion segmented flow, which is being actively developed[139].

Time-domain multiplex
A method of interfacing a certain number of coils with a smaller number of receive channels for parallelizing multiple NMR experiments.

Single-scan 2D NMR

The 2D — and, in general, *n*D — NMR information originating from conventional and from single-shot acquisitions should be equivalent in terms of peak positions, line shapes, spectral resolution and intensities[140]. In practice, however, the need to constantly apply magnetic field gradients to define the encoding and read-out spectral characteristics imparts constraints to the single-scan acquisition methods. For instance, gradient-based manipulations, and in particular those relying on strong gradients applied over tens to hundreds of milliseconds, will only work if high-quality gradient coils and amplifiers are employed. Such quality is routinely achieved by human MRI scanners as it is essential for their operation; the same is not always the case for high-resolution NMR, where gradient quality and agility have not been given the highest priority. This, in turn, leads to special requirements for phasing the data, setting up suitable spectral widths and so on[141]. However, the most important limitation of ultra-fast nD NMR pertains to sensitivity and the presence of added noise.

In conventional NMR acquisitions, noise will be determined by how much the receiver's bandwidth is opened — the noise voltage increasing, in general, as √bandwidth. This bandwidth will be given by the

inverse of the acquisition dwell time (that is, the time between sampled data points), which in conventional 2D NMR is $1/\Delta t_2$ (REFS[17,89]). In ultra-fast NMR, however, the full F_1 indirect-domain information is to be contained within each dwell time Δt_2; for acquisitions aiming at defining the F_1 domain with N_1 equidistantly sampled k-domain points, the receiving bandwidth will thus have to be opened up by an additional N_1 factor over its conventional counterpart, in order to capture these changes. This leads to S/N per scan decreasing by $\sqrt{N_1}$ over such a conventional counterpart. This is a sensitivity penalty that will increase as the number of indirect domains that are spatio-temporally encoded increases — as each such additional sampled domain will have to be collected within each direct-domain acquisition dwell time. In cases where sensitivity is not a limiting factor, for example when dealing with sufficiently concentrated samples, this may be acceptable. But when dealing with sensitivity-limited samples, this price can be particularly onerous.

The sensitivity of single-shot 2D NMR can be improved by signal averaging in different forms — be it collecting the same scan over and over, interleaving the data so as to reduce the gradient's demands[8] or performing ≥3D NMR acquisitions employing mixed temporal and spatio-temporal encodings[142] (in this latter case, the t_3 temporal encoding provides a sort of signal averaging). Special cases where a priori information is known — for instance, an F_1 spectral region that is known to be devoid of resonances and, hence, in no need of sampling — can be alleviated from the full, stringent sampling demands mentioned above. In such instances, the effective number N_1 of points sampled can be de facto reduced, leading to improved sensitivity. Another way to alleviate these sampling-derived demands could involve the use of multiple high-quality (micro)coils and receivers, leading to savings in the sampling requirements that are analogous to those enjoyed by parallel receiving in MRI. Such concepts, however, remain to be tested in the domain of high-resolution spectroscopy.

Optimizing multi-FID detection schemes

The same number of FIDs must be acquired for every module in a parallelized multi-FID experiment, meaning the minimum experiment time is necessarily limited by the least sensitive module. In practice, the time savings realized may not be as great, particularly for low-concentration samples that require many transients for the least sensitive module but not for others. It is possible to increase the number of scans only for the least sensitive module with a corresponding reduction in the number of t_1 increments to trade resolution for sensitivity[143]. However, this is limited to situations where high spectral resolution is not required for the least sensitive module, which is most often the case for ^{15}N correlations of small molecules. In cases of high sensitivity, benefits can be realized through the incorporation of non-uniform sampling schemes[144], either to afford additional time savings or to increase resolution in indirect dimensions without extending experiment durations[57].

The use of the same magnetization pool multiple times can also lead to drops in performance. This is most obvious in polarization sharing experiments, where R_S is necessarily lower than one. However, this can also inadvertently arise in NOAH supersequences involving the HMBC module, which destroys the bulk magnetization required for any subsequent homonuclear module. For example, the NOAH-3 BSC supersequence[53,57] (HMBC/HSQC/COSY) recorded on a sample of the cyclosporine in benzene-d_6 has $\rho_t = 2.65$ and $R_S = 1.0$, 0.92 and 0.27 for the three modules respectively, leading to $\varepsilon_t = 1.63$, 1.50 and 0.44 (E.K., J.R.J.Y. & T.D.W.C., unpublished work). The observed COSY signal in this case derives from magnetization that was excited during the HMBC module but has only partially recovered during the two subsequent FID periods prior to its use in the COSY. Nevertheless, this decrease in R_S is readily tolerated, as the COSY spectrum is naturally far more intense than the HMBC. A more insidious problem arises from the differing relaxation rates of the different protons in the sample, leading to imbalanced cross-peak intensities

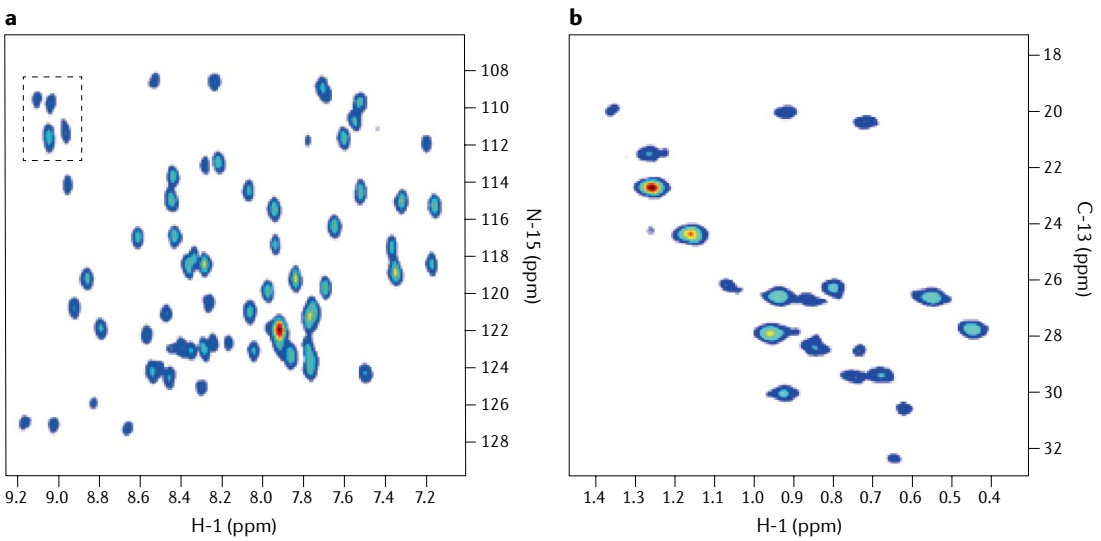

Fig. 11 | **Single-shot 2D NMR spectra. a** | ^{15}N–^{1}H HSQC spectrum of ubiquitin. **b** | ^{13}C-^{1}H HMQC spectrum of the methyl region of protein A. Acquired in <80 ms.

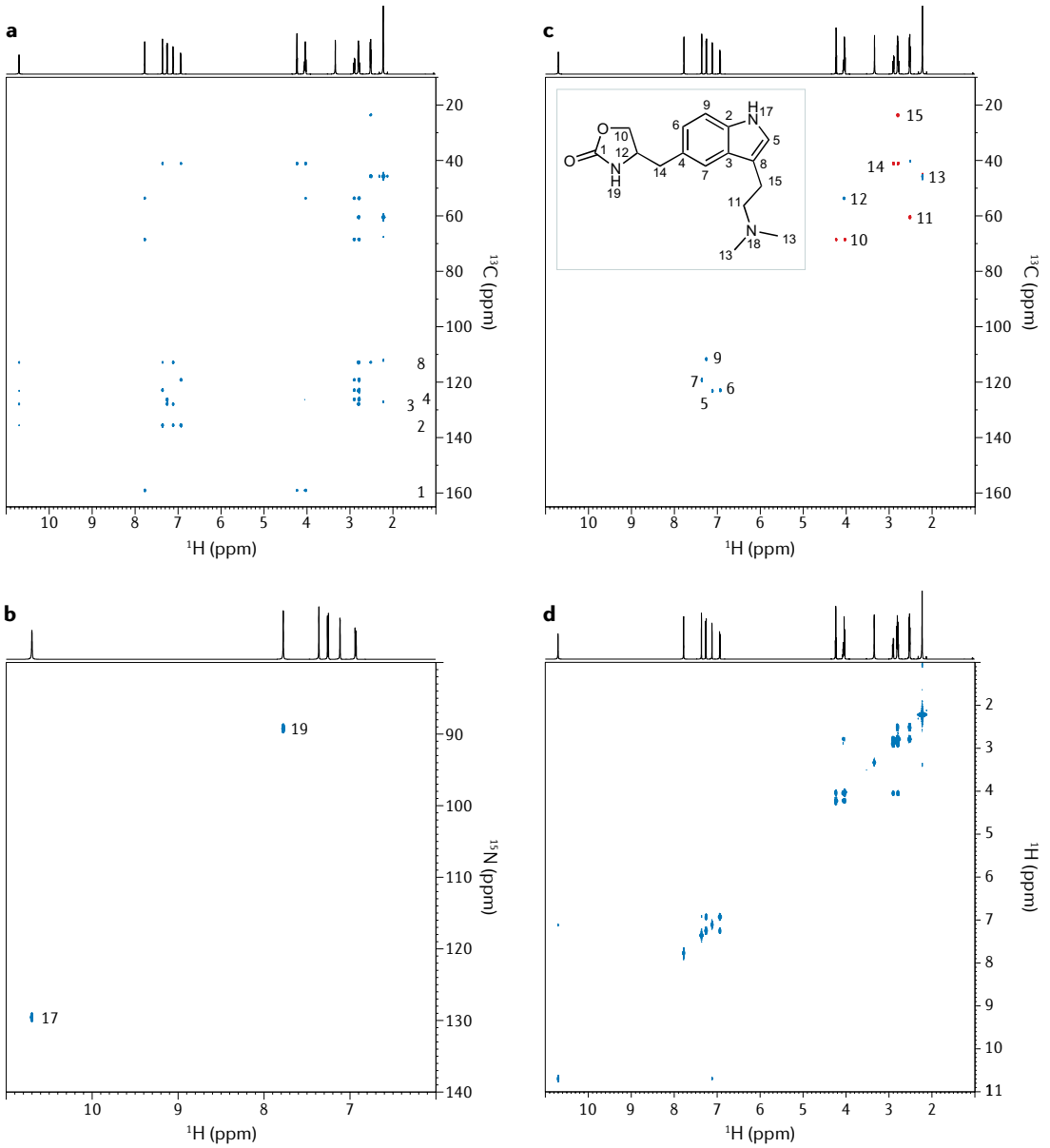

Fig. 12 | **NOAH data recorded for the pharmaceutical zolmitriptan. a–d** | Spectra recorded using the NOAH-4 BMSC sequence illustrated in FIG. 4d. This supersequence yields the four following spectra: ^{1}H–^{13}C HMBC (panel **a**), ^{1}H–^{15}N HMQC (panel **b**), ^{1}H–^{13}C multiplicity edited HSQC (panel **c**) and ^{1}H–^{1}H COSY (panel **d**). Inset: CASE (computer-assisted structure elucidation)-derived structure and assignments in order of decreasing ^{13}C chemical shift. Duration of NOAH BMSC was 20 min 12 s, whereas the sum for the four conventional two-dimensional (2D) experiments was 60 min 9 s ($\rho_t = 2.98$). Data collected on a 50 mM zolmitriptan sample in DMSO using a Bruker AVIII 700 equipped with a TCI H/C/N cryoprobe, with two transients, recovery period $d_1 = 1.5$ s and 256 t_1 increments per module; t_1 is the time period associated with the indirectly encoded frequency dimension. Parameters optimized for $^{1}J_{CH} = 145$ Hz, $^{n}J_{CH} = 8$ Hz, $^{1}J_{NH} = 90$ Hz. CASE structure generated using Bruker CMC-SE software.

in the COSY module. This can, however, be ameliorated by inserting a period of isotropic mixing prior to the COSY[53,145,146], which serves to rebalance the available magnetization across all protons in the manner of the ASAP (acceleration through sharing of adjacent polarization) experiments[147–149].

Balancing the sensitivities in multi-receiver experiments involving insensitive and diluted nuclei such as ^{13}C, ^{15}N and ^{29}Si is a significant challenge, particularly in low-concentration samples. Probes optimized for direct detection of such nuclei are essential in multinuclear detected experiments. Instrument software can also impose limits on method development. For example, the commercial Bruker software TopSpin limits the number of memory blocks, and hence NOAH modules, to five. This limit has been reached and should be at least doubled to allow design and recording of experiments similar to the extended PANACEA pulse scheme.

Outlook

Although the advantages of parallelization have been realized in many fields of science and technology, including MRI[2–4], NMR parallelization has not yet reached its full potential. We have discussed the basic parallelization

approaches that have been developed in NMR over the past decade and their significant gains in speed and sensitivity. Many of these techniques are still under active development, with new methods continually being demonstrated[7,13,16,31,55,83]. However, the largest gains are expected to emerge once the techniques discussed in this Primer are combined to multiply the benefits of individual approaches.

One of the major advances in multiple microcoil NMR that can be envisioned is the use of 3D microfabrication techniques to improve the quality and reproducibility of the detector set-up used for data acquisition[150,151]. Most of the studies outlined in this Primer have used radiofrequency coils wound by hand, with discrete capacitors used for impedance matching: as such, these are very labour intensive to produce, and there is considerable inter-element variability in performance. Microfabrication techniques are much more accurate and reproducible, with the proviso that the conductor thickness needs to be much greater than typically used in this type of manufacturing, otherwise the coil resistance at high frequencies will be very large and *S*/*N* will be correspondingly reduced. In addition, it should be possible to integrate much of the electronic circuits used for signal detection and demodulation very close to the radiofrequency coil, which will improve performance. Another potential application is in the field of metabolomics, which studies enormous numbers of samples. The time required could be reduced significantly by, for example, running several samples simultaneously using the multiple microcoil technology.

The existing approaches towards time-shared and multiple-FID experiments lead to significant reductions in experiment time and improved sensitivity per unit time relative to conventional experiments[54]. However, the manipulation of multiple magnetization components typically requires the introduction of additional pulse sequence elements, reducing efficiency owing to instrumental imperfections[152]. An immediate challenge is therefore the design of improved pulse sequences that have comparable or enhanced performance relative to conventional experiments, for example, through optimal control theory[153–155].

The extension of these techniques to higher-dimensional experiments is an obvious area for future development. Although time-shared 3D and 4D sequences have long been used in biomolecular NMR[156–158], there has been much less work on sequential and multinuclear acquisition experiments[76,77,96]. The potential time savings realized through these would be even more substantial than for their 2D counterparts.

The combination of different approaches to parallelized acquisition provides a fertile area for future investigation. For example, one may even envision experiments in which separate magnetization pools can be sampled in an interleaved fashion without any explicit recovery delays. This can be easily done when detecting multiple nuclei, but the homonuclear case is substantially more difficult owing to the precise control required over each magnetization pool. Marrying multi-FID schemes with spatial encoding could enable rapid and continuous sampling of magnetization pools for even greater gains in time efficiency and sensitivity per unit time.

In the area of multinuclear, multi-receiver detection, the very different intrinsic sensitivities of diluted nuclei such as ^{13}C, ^{15}N and ^{29}Si and similar versus high γ nuclei such as ^{1}H and ^{19}F present significant challenges, particularly in low-concentration samples. Probes optimized for direct detection of such nuclei are essential. For instance, the best performance of parallel NMR experiments that are based on direct detection of ^{13}C is achieved with cryoprobes that are designed to maximize the ^{13}C sensitivity. Constructing radiofrequency coils from high-temperature superconductors roughly doubles the sensitivity of cryogenic probes. For example, a home-built 1.5-mm (35 µl) high-temperature superconductor probe optimized for ^{13}C detection improved sensitivity by a factor of >20 compared with a commercial room-temperature probe for the same sample mass[70], thus reducing the measurement time for small sample quantities by a factor of >4,000. It is expected that future probe developments and advances in hyperpolarization techniques will make ^{13}C-detected experiments such as PANACEA more practical. For instance, hyperpolarization allowed the recording of INADEQUATE spectra at the natural abundance of ^{13}C in a single scan[159].

Parallelized experiments could also be employed for monitoring time-dependent processes such as chemical reactions to alleviate the spectral crowding and associated ambiguities in interpreting conventional 1D methods. Furthermore, the use of multi-FID pulse schemes in conjunction with time-resolved non-uniform sampling[160] or ultra-fast methodology is extremely promising, but has yet to be investigated. Further development of ultra-fast supersequences including direct detection of nuclei other than protons also offers promise in structure characterization and reaction monitoring, with ^{19}F offering applications in fluorine chemistry and drug design. Combining multiple microcoil technology with efficient NMR supersequences would produce unprecedented throughput capability. Likewise, merging the ultra-fast methodology with various pulse schemes for structure elucidation from a single measurement, such as NOAH and PANACEA, opens amazing opportunities to design experiments yielding organic molecule structures in a fraction of a second.

In conclusion, parallelization in NMR enables several concepts in hardware, data acquisition and data processing to be co-developed in ways in which the total gain is greater than the sum of the parts. There is a strong analogy with MRI, where recent advances in rapid patient imaging using massively undersampled data and the introduction of artificial intelligence into data processing have only been made possible by the availability of parallel data acquisition. We hope that future researchers will look back on the days of a single-sample/single-experiment mode in the way that we currently remember the early days of NMR where spectra were laboriously collected by sweeping across the entire frequency range one step at a time.

Published online: 08 April 2021

1. Tucker, T., Marra, M. & Friedman, J. M. Massively parallel sequencing: the next big thing in genetic medicine. *Am. J. Hum. Genet.* **85**, 142–154 (2009).
2. Roemer, P. B., Edelstein, W. A., Hayes, C. E., Souza, S. P. & Mueller, O. M. The NMR phased array. *Magn. Reson. Med.* **16**, 192–225 (1990).
3. Pruessmann, K. P., Weiger, M., Scheidegger, M. B. & Boesiger, P. SENSE: sensitivity encoding for fast MRI. *Magn. Reson. Med.* **42**, 952–962 (1999).
4. Griswold, M. A. et al. Generalized autocalibrating partially parallel acquisitions (GRAPPA). *Magn. Reson. Med.* **47**, 1202–1210 (2002).
5. Webb, A. G., Sweedler, J. V. & Raftery, D. in *On-Line LC-NMR and Related Techniques* (ed. Albert, K.) 259–279 (Wiley, 2002).
6. Webb, A. G. Radiofrequency microcoils for magnetic resonance imaging and spectroscopy. *J. Magn. Reson.* **229**, 55–66 (2013).
7. Frydman, L., Scherf, T. & Lupulescu, A. The acquisition of multidimensional NMR spectra within a single scan. *Proc. Natl Acad. Sci. USA* **99**, 15858–15862 (2002).
This paper introduces the basic idea underlying the execution of 2D NMR acquisitions in a single shot by spatio-temporal encoding.
8. Gal, M. & Frydman, L. in *Multidimensional NMR Methods for the Solution State* (eds Morris, G. A. & Emsley, J. W.) 43–60 (Wiley, 2009).
This paper includes numerous practical details on how to set up and process 2D homonuclear and heteronuclear NMR acquisitions in commercial spectrometers.
9. Mishkovsky, M. & Frydman, L. Principles and progress in ultrafast multidimensional nuclear magnetic resonance. *Ann. Rev. Phys. Chem.* **60**, 429–448 (2009).
10. Tal, A. & Frydman, L. Single-scan multidimensional magnetic resonance. *Progr. NMR Spectrosc.* **57**, 241–292 (2010).
This paper contains descriptions of the physical principles underlying the main tools involved in single-scan spatio-temporally encoded NMR and MRI, paying attention to the effects of the frequency-swept manipulations underlying these experiments.
11. Giraudeau, P. & Frydman, L. Ultrafast 2D NMR: an emerging tool in analytical spectroscopy. *Ann. Rev. Anal. Chem.* **7**, 129–161 (2014).
This paper highlights various applications enabled by single-scan 2D NMR for chemical and biophysical scenarios.
12. Ardenkjaer-Larsen, J. H. et al. Increase in signal-to-noise ratio of >10,000 times in liquid-state NMR. *Proc. Natl Acad. Sci. USA* **100**, 10158–10163 (2003).
13. Kupče, Ē., Freeman, R. & John, R. B. K. Parallel acquisition of two-dimensional NMR spectra of several nuclear species. *J. Am. Chem. Soc* **128**, 9606–9607 (2006).
This paper introduces the direct multinuclear detection and parallel NMR spectroscopy (PANSY) technique, with PANSY–COSY and HETCOR/TOCSY experiments used as a proof of principle.
14. Kovacs, H. & Kupče, Ē. Parallel NMR spectroscopy with simultaneous detection of ^{1}H and ^{19}F nuclei. *Magn. Reson. Chem.* **54**, 544–560 (2016).
This paper modifies various conventional small-molecule experiments to include direct multinuclear detection involving protons and ^{19}F. Basic principles of multinuclear detection techniques are discussed.
15. Nolis, P., Pérez-Trujillo, M. & Parella, T. Multiple FID acquisition of complementary HMBC data. *Angew. Chem. Int. Ed.* **46**, 7495–7497 (2007).
16. Kupče, Ē. & Claridge, T. D. W. NOAH: NMR supersequences for small molecule analysis and structure elucidation. *Angew. Chem. Int. Ed.* **56**, 11779–11783 (2017).
This paper introduces the NOAH technique, and describes how various heteronuclear and homonuclear 2D NMR experiments can be combined into a supersequence by careful manipulation of magnetization pools.
17. Ernst, R. R., Bodenhausen, G. & Wokaun, A. *Principles of Nuclear Magnetic Resonance in One and Two Dimensions* 148–158 (Oxford Univ. Press, 1987).
18. deGraaf, R. A. *In Vivo NMR Spectroscopy, Principles and Techniques* 6–8 (Wiley, 1998).
19. Kovacs, H., Moskau, D. & Spraul, M. Cryogenically cooled probes — a leap in NMR technology. *Prog. NMR Spectrosc.* **46**, 131–155 (2005).
20. Martin, G. E. Small-sample cryoprobe NMR applications. *Encycl. Magnetic Reson.* https://doi.org/10.1002/9780470034590.emrstm1300 (2012).
21. Cheatham, S., Gierth, P., Bermel, W. & Kupče, Ē. HCNMBC — a pulse sequence for H–(C)–N multiple bond correlations at natural isotopic abundance. *J. Magn. Reson.* **247**, 38–41 (2014).
22. Aramini, J. M., Rossi, P., Anklin, C., Xiao, R. & Montelione, G. T. Microgram-scale protein structure determination by NMR. *Nat. Methods* **4**, 491–493 (2007).
23. MacNamara, E., Hou, T., Fisher, G., Williams, S. & Raftery, D. Multiplex sample NMR: an approach to high-throughput NMR using a parallel coil probe. *Anal. Chim. Acta.* **397**, 9–16 (1999).
This paper shows for the first time that multiple samples can be studied at once using an arrangement in which radiofrequency coils are connected in parallel.
24. Hou, T., Smith, J., MacNamara, E., Macnaughtan, M. & Raftery, D. Analysis of multiple samples using multiplex sample NMR: selective excitation and chemical shift imaging approaches. *Anal. Chem.* **73**, 2541–2546 (2001).
25. Macnaughtan, M. A., Hou, T., Xu, J. & Raftery, D. High-throughput nuclear magnetic resonance analysis using a multiple coil flow probe. *Anal. Chem.* **75**, 5116–5123 (2003).
26. Macnaughtan, M. A., Hou, T., MacNamara, E., Santini, R. & Raftery, D. NMR difference probe: a dual-coil probe for NMR difference spectroscopy. *J. Magn. Reson.* **156**, 97–103 (2002).
27. Dumez, J.-N. Spatial encoding and spatial selection methods in high-resolution NMR spectroscopy. *Prog. Nucl. Magn. Reson. Spectrosc.* **116**, 101–134 (2018).
28. Loening, N. M., Thrippleton, M. J., Keeler, J. & Griffin, R. G. Single-scan longitudinal relaxation measurements in high-resolution NMR spectroscopy. *J. Magn. Reson.* **164**, 321–328 (2003).
29. Pelta, M. D., Morris, G. A., Stchedroff, M. J. & Hammond, S. J. A one-shot sequence for high-resolution diffusion-ordered spectroscopy. *Magn. Reson. Chem.* **40**, S147–S152 (2002).
30. Zangger, K. Pure shift NMR. *Prog. Nucl. Magn. Reson. Spectrosc.* **86–87**, 1–20 (2015).
31. Li, Y., Wolters, A., Malaway, P., Sweedler, J. V. & Webb, A. G. Multiple solenoidal microcoil probes for high-sensitivity, high-throughput nuclear magnetic resonance spectroscopy. *Anal. Chem.* **71**, 4815–4820 (1999).
This paper is the first to demonstrate that multiple independent coils and samples can be used to acquire high-resolution NMR spectra with full efficiency and *S*/*N*.
32. Zhang, X., Sweedler, J. V. & Webb, A. G. A probe design for the acquisition of homonuclear, heteronuclear, and inverse detected NMR spectra from multiple samples. *J. Magn. Reson.* **153**, 254–258 (2001).
This paper is the first to show that heteronuclear 2D NMR spectra can be obtained from different protein samples simultaneously.
33. Wang, H., Ciobanu, L., Edison, A. S. & Webb, A. G. An eight-coil high-frequency probehead design for high-throughput nuclear magnetic resonance spectroscopy. *J. Magn. Reson.* **170**, 206–212 (2004).
34. Wolters, A. M., Jayawickrama, D. A., Webb, A. G. & Sweedler, J. V. NMR detection with multiple solenoidal microcoils for continuous-flow capillary electrophoresis. *Anal. Chem.* **74**, 5550–5555 (2002).
35. Ciobanu, L., Jayawickrama, D. A., Zhang, X., Webb, A. G. & Sweedler, J. V. Measuring reaction kinetics by using multiple microcoil NMR spectroscopy. *Angew. Chem. Int. Ed.* **42**, 4669–4672 (2003).
36. Frydman, L., Lupulescu, A. & Scherf, T. Principles and features of single-scan two-dimensional NMR spectroscopy. *J. Am. Chem. Soc.* **125**, 9204–9217 (2003).
37. Shrot, Y. & Frydman, L. Single-scan NMR spectroscopy at arbitrary dimensions. *J. Am. Chem. Soc.* **125**, 11385–11396 (2003).
38. Jeener, J. Pulse pair technique in high resolution NMR. Lecture presented at Ampere International Summer School II, Basko Polje, Yugoslavia (1971).
39. Aue, W. P., Bartholdi, E. & Ernst, R. R. Two-dimensional spectroscopy. Application to nuclear magnetic resonance. *J. Chem. Phys.* **64**, 2229–2246 (1976).
40. Mansfield, P. Spatial mapping of the chemical shift in NMR. *Magn. Reson. Med.* **1**, 370–386 (1984).
41. Smith, P. E. S. et al. T1 relaxation measurements: probing molecular properties in real time. *ChemPhysChem* **14**, 3138–3145 (2013).
42. Shrot, Y. & Frydman, L. Single scan 2D DOSY NMR. *J. Magn. Reson.* **195**, 226–231 (2008).
43. Shrot, Y. & Frydman, L. The effects of molecular diffusion in single-scan 2D NMR. *J. Chem. Phys.* **128**, 164513 (2008).
44. Yon, M. et al. Diffusion tensor distribution imaging of an in vivo mouse brain at ultra-high magnetic field by spatiotemporal encoding. *NMR Biomed*, **33**, e4355 (2020).
45. Solomon, E. et al. Diffusion-weighted MR breast imaging with submillimeter resolution and immunity to artifacts by spatio-temporal encoding at 3T. *Magn. Reson. Med.* **84**, 1391–1403 (2020).
46. Bao, Q., Solomon, E., Liberman, G. & Frydman, L. High-resolution diffusion MRI studies of development in pregnant mice visualized by novel spatiotemporal encoding schemes. *NMR Biomed.* **33**, e4208 (2020).
47. Cousin, S. F., Liberman, G., Solomon, E., Otikovs, M. & Frydman, L. A regularized reconstruction pipeline for high definition diffusion MRI in challenging regions incorporating a per-shot image correction. *Magn. Reson. Med.* **81**, 3080–3093 (2019).
48. Liberman, G., Solomon, E., Lustig, M. & Frydman, L. Mulitple coil *k*-space interpolation enhances resolution in single-shot spatiotemporal MRI. *Magn. Reson. Med.* **79**, 796–805 (2018).
49. Solomon, E., Liberman, G., Zhang, Z. & Frydman, L. Diffusion MRI measurements in challenging head and brain regions via cross-term spatiotemporally encoding. *Sci. Rep.* **7**, 18010 (2017).
50. Garbow, J. R., Weitekamp, D. P. & Pines, A. Bilinear rotation decoupling of homonuclear scalar interactions. *Chem. Phys. Lett.* **93**, 504–509 (1982).
51. Wimperis, S. & Freeman, R. An excitation sequence which discriminates between direct and long-range CH coupling. *J. Magn. Reson.* **58**, 348–353 (1984).
52. Briand, J. & Sørensen, O. W. Simultaneous and independent rotations with arbitrary flip angles and phases for I, IS$^{\alpha}$, and IS$^{\beta}$ spin systems. *J. Magn. Reson.* **135**, 44–49 (1998).
53. Kupče, Ē. & Claridge, T. D. W. Molecular structure from a single NMR supersequence. *Chem. Commun.* **54**, 7139–7142 (2018).
This paper is the first demonstration of how parallelized NMR experiments can be combined with computer-assisted structural elucidation, allowing unknown molecular frameworks to be determined in a far shorter time than previously possible.
54. Kupče, Ē. & Claridge, T. D. W. New NOAH modules for structure elucidation at natural isotopic abundance. *J. Magn. Reson.* **307**, 106568 (2019).
55. Parella, T. & Nolis, P. Time-shared NMR experiments. *Concepts Magn. Reson.* **36A**, 1–23 (2010).
This review on time-shared sequences with a focus on small-molecule applications goes into detail about sensitivity considerations as well as numerous experimental variants and improvements on the basic time-shared concept.
56. Sørensen, O. W. Aspects and prospects of multidimensional time-domain spectroscopy. *J. Magn. Reson.* **89**, 210–216 (1990).
57. Claridge, T. D. W., Mayzel, M. & Kupče, Ē. Triplet NOAH supersequences optimised for small molecule structure characterisation. *Magn. Reson. Chem.* **57**, 946–952 (2019).
58. Kakita, V. M. R., Rachineni, K., Bopardikar, M. & Hosur, R. V. NMR supersequences with real-time homonuclear broadband decoupling: sequential acquisition of protein and small molecule spectra in a single experiment. *J. Magn. Reson.* **297**, 108–112 (2018).
59. Kakita, V. M. R. & Hosur, R. V. All-in-one NMR spectroscopy of small organic molecules: complete chemical shift assignment from a single NMR experiment. *RSC Adv.* **10**, 21174–21179 (2020).
60. Cavanagh, J. & Rance, M. Sensitivity-enhanced NMR techniques for the study of biomolecules. *Annu. Rep. NMR Spectrosc.* **27**, 1–58 (1993).
61. Palmer, A. G., Cavanagh, J., Wright, P. E. & Rance, M. Sensitivity improvement in proton-detected two-dimensional heteronuclear correlation NMR spectroscopy. *J. Magn. Reson.* **93**, 151–170 (1991).
62. Cavanagh, J. & Rance, M. Sensitivity improvement in isotropic mixing (TOCSY) experiments. *J. Magn. Reson.* **88**, 72–85 (1990).
63. Nolis, P., Motiram-Corral, K., Pérez-Trujillo, M. & Parella, T. Interleaved dual NMR acquisition of equivalent transfer pathways in TOCSY and HSQC experiments. *ChemPhysChem* **20**, 356–360 (2019).

64. Nolis, P. & Parella, T. Practical aspects of the simultaneous collection of COSY and TOCSY spectra. *Magn. Reson. Chem.* **57**, S85–S94 (2019).
65. Nolis, P., Motiram-Corral, K., Pérez-Trujillo, M. & Parella, T. Simultaneous acquisition of two 2D HSQC spectra with different ^{13}C spectral widths. *J. Magn. Reson.* **300**, 1–7 (2019).
66. Nagy, T. M., Kövér, K. E. & Sørensen, O. W. Double and adiabatic BANGO for concatenating two NMR experiments relying on the same pool of magnetization. *J. Magn. Reson.* **316**, 106767 (2020).
67. Motiram-Corral, K., Pérez-Trujillo, M., Nolis, P. & Parella, T. Implementing one-shot multiple-FID acquisition into homonuclear and heteronuclear NMR experiments. *Chem. Commun.* **54**, 13507–13510 (2018).
68. Bermel, W., Bertini, I., Felli, I. C., Piccioli, M. & Pierattelli, R. ^{13}C-detected protonless NMR spectroscopy of proteins in solution. *Prog. NMR Spectrosc.* **48**, 25–45 (2006).
69. Pervushin, K., Vögeli, B. & Eletsky, A. Longitudinal ^{1}H relaxation optimization in TROSY NMR spectroscopy. *J. Am. Chem. Soc.* **124**, 12898–12902 (2002).
70. Edison, A. S., Le Guennec, A., Delaglio F. & Kupče, Ē. in *NMR-based Metabolomics: Methods and Protocols* (eds Gowda, G. A. N. & Raftery, D.) 69–96 (Humana Press, 2019).
71. Kupče, Ē. & Freeman, R. Molecular structure from a single NMR sequence (fast-PANACEA). *J. Magn. Reson.* **206**, 147–153 (2010).
72. van de Ven, F. J. M. *Multidimensional NMR in Liquids—Basic Principles and Experimental Methods* 165–171 (VCH, 1995).
73. Kitevski-LeBlanc, J. L. & Prosser, R. S. Current applications of ^{19}F NMR to studies of protein structure and dynamics. *Prog. NMR Spectrosc.* **62**, 1–33 (2012).
74. Wan, Y.-B. & Li, X.-H. Two-dimensional nuclear magnetic resonance spectroscopy with parallel acquisition of ^{1}H–^{1}H and ^{19}F–^{19}F correlations. *Chin. J. Anal. Chem.* **43**, 1203–1209 (2015).
75. Gonen, O. et al. Simultaneous and interleaved multinuclear chemical-shift imaging, a method for concurrent, localized spectroscopy. *J. Magn. Reson.* **104B**, 26–33 (1994).
76. Bellstedt, P. et al. Sequential acquisition of multi-dimensional heteronuclear chemical shift correlation spectra with ^{1}H detection. *Sci. Rep.* **4**, 4490 (2014).
77. Wiedemann, C. et al. Sequential protein NMR assignments in the liquid state via sequential data acquisition. *J. Magn. Reson.* **239**, 23–28 (2014).
78. Gierth, P., Codina, A., Schumann, F., Kovacs, H. & Kupče, Ē. Fast experiments for structure elucidation of small molecules: Hadamard NMR with multiple receivers. *Magn. Reson. Chem.* **53**, 940–944 (2015).
79. Pudakalakatti, S. M. et al. A fast NMR method for resonance assignments: application to metabolomics. *J. Biomol. NMR* **58**, 165–173 (2014).
80. Pudakalakatti, S. M., Dubey, A. & Atreya, H. S. Simultaneous acquisition of three NMR spectra in a single experiment for rapid resonance assignments in metabolomics. *J. Chem. Sci.* **127**, 1091–1097 (2015).
81. Kupče, Ē. & Freeman, R. Resolving ambiguities in two-dimensional NMR spectra: the 'TILT' experiment. *J. Magn. Reson.* **172**, 329–332 (2005).
82. Freeman, R. & Kupče, Ē. Distant echoes of the accordion: reduced dimensionality, GFT-NMR, and projection-reconstruction of multidimensional spectra. *Concepts Magn. Reson.* **23A**, 63–75 (2008).
83. Kupče, Ē. & Freeman, R. Molecular structure from a single NMR experiment. *J. Am. Chem. Soc* **130**, 10788–10792 (2008).
This paper introduces the idea of constructing the PANACEA pulse scheme that allows the structure of small organic molecules to be determined unambiguously from a single NMR experiment.
84. Bax, A., Freeman, R. & Kempsell, S. P. Natural abundance carbon-13–carbon-13 coupling observed via double-quantum coherence. *J. Am. Chem. Soc.* **102**, 4849–4851 (1980).
85. Meissner, A. & Sørensen, O. W. Exercise in modern NMR pulse sequence design: INADEQUATE CR. *Concepts Magn. Reson.* **14**, 141–154 (2002).
86. Kupče, Ē., Nishida, T. & Freeman, R. Hadamard NMR spectroscopy. *Prog. NMR Spectrosc.* **42**, 95–122 (2003).
87. Jeannerat, D. Rapid multidimensional NMR: high resolution by spectral aliasing. *Ency. Magn. Reson.* https://doi.org/10.1002/9780470034590.emrstm1187 (2011).
88. Kupče, Ē. & Wrackmeyer, B. Multiple receiver experiments for NMR spectroscopy of organosilicon compounds. *Appl. Organometal. Chem.* **24**, 837–841 (2010).
89. Claridge, T. D. W. *High-resolution NMR Techniques in Organic Chemistry* 3rd edn 171–202 (Elsevier, 2016).
90. Elyashberg, M. E., Williams, A. J. & Martin, G. E. Computer-assisted structure verification and elucidation tools in NMR-based structure elucidation. *Prog. NMR Spectrosc.* **53**, 1–104 (2008).
91. Sattler, M., Maurer, M., Schleucher, J. & Griesinger, C. A simultaneous ^{15}N,^{1}H- and ^{13}C,^{1}H-HSQC with sensitivity enhancement and a heteronuclear gradient echo. *J. Biomol. NMR* **5**, 97–102 (1995).
This paper is an early demonstration of how simultaneous acquisition can be used to accelerate acquisition of heteronuclear correlation spectra, and also provides an illuminating discussion of the theory underpinning the construction of pulse sequence elements for time-shared experiments.
92. Nolis, P., Pérez-Trujillo, M. & Parella, T. Time-sharing evolution and sensitivity enhancements in 2D HSQC–TOCSY and HSQMBC experiments. *Magn. Reson. Chem.* **44**, 1031–1036 (2006).
93. Haasnoot, C. A. G., van de Ven, F. J. M. & Hilbers, C. W. COCONOSY. Combination of 2D correlated and 2D nuclear Overhauser enhancement spectroscopy in a single experiment. *J. Magn. Reson.* **56**, 343–349 (1984).
94. Gurevich, A. Z., Barsukov, I. L., Arseniev, A. S. & Bystrov, V. F. Combined COSY–NOESY experiment. *J. Magn. Reson.* **56**, 471–478 (1984).
95. Viegas, A. et al. UTOPIA NMR: activating unexploited magnetization using interleaved low-gamma detection. *J. Biomol. NMR* **64**, 9–15 (2016).
96. Schiavina, M. et al. Taking simultaneous snapshots of intrinsically disordered proteins in action. *Biophys. J.* **117**, 46–55 (2019).
97. Kupče, Ē. & Freeman, R. High-resolution NMR correlation experiments in a single measurement (HR-PANACEA). *Magn. Reson. Chem.* **48**, 333–336 (2010).
98. Giraudeau, P., Shrot, Y. & Frydman, L. Multiple ultrafast, broadband 2D NMR spectra of hyperpolarized natural products. *J. Am. Chem. Soc.* **131**, 13902–13903 (2009).
99. Donovan, K. J., Kupče, Ē. & Frydman, L. Multiple parallel 2D NMR acquisitions in a single scan. *Angew. Chem. Int. Ed.* **52**, 4152–4155 (2013).
100. Purea, A., Neuberger, T. & Webb, A. G. Simultaneous NMR microimaging of multiple single-cell samples. *Concepts Magn. Reson.* **22B**, 7–14 (2004).
101. Lee, H., Sun, E., Ham, D. & Weissleder, R. Chip-NMR biosensor for detection and molecular analysis of cells. *Nat. Med.* **14**, 869–874 (2008).
102. Shapira, B., Shetty, K., Brey, W. W., Gan, Z. & Frydman, L. Single scan 2D NMR spectroscopy on a 25 T bitter magnet. *Chem. Phys. Lett.* **442**, 478–482 (2007).
103. Gal, M., Mishkovsky, M. & Frydman, L. Real-time monitoring of chemical transformations by ultrafast 2D NMR spectroscopy. *J. Am. Chem. Soc.* **128**, 951–956 (2006).
104. Herrera, A. et al. Real-time monitoring of organic reactions with two-dimensional ultrafast TOCSY NMR spectroscopy. *Angew. Chem. Int. Ed.* **48**, 6274–6277 (2009).
105. Pardo, Z. D. et al. Monitoring mechanistic details in the synthesis of pyrimidines via real-time, ultrafast multidimensional NMR spectroscopy. *J. Am. Chem. Soc.* **134**, 2706–2715 (2012).
106. Queiroz, L. H. K. Jr., Giraudeau, P., dos Santos, F. A. B., Oliveira, K. T. & Ferreira, A. G. Real-time mechanistic monitoring of an acetal hydrolysis using ultrafast 2D NMR. *Magn. Reson. Chem.* **50**, 496–501 (2012).
107. Gal, M., Schanda, P., Brutscher, B. & Frydman, L. UltraSOFAST HMQC NMR and the repetitive acquisition of 2D protein spectra at Hz rates. *J. Am. Chem. Soc.* **129**, 1372–1377 (2007).
108. Gal, M., Kern, T., Schanda, P., Frydman, L. & Brutscher, B. An improved ultrafast 2D NMR experiment: towards atom-resolved real-time studies of protein kinetics at multi-Hz rates. *J. Biomol. NMR.* **43**, 1–10 (2009).
109. Shapira, B., Karton, A., Aronzon, D. & Frydman, L. Real-time 2D NMR identification of analytes undergoing continuous chromatographic separation. *J. Am. Chem. Soc.* **126**, 1262–1265 (2004).
110. Queiroz, L. H. K. Jr., Queiroz, D. P. K., Dhooghe, L., Ferreira, A. G. & Giraudeau, P. Real-time separation of natural products by ultrafast 2D NMR coupled to on-line HPLC. *Analyst* **137**, 2357–2361 (2012).
111. Shapira, B., Morris, E., Muszkat, A. K. & Frydman, L. Sub-second 2D NMR spectroscopy at sub-mM concentrations. *J. Am. Chem. Soc.* **126**, 11756–11757 (2004).
112. Frydman, L. & Blazina, D. Ultrafast two-dimensional nuclear magnetic resonance spectroscopy of hyperpolarized solutions. *Nat. Phys.* **3**, 415–419 (2007).
113. Mishkovsky, M. & Frydman, L. Progress in hyperpolarized ultrafast 2D NMR spectroscopy. *ChemPhysChem.* **9**, 2340–2348 (2008).
114. Lloyd, L. S. et al. Utilization of SABRE-derived hyperpolarization to detect low-concentration analytes via 1D and 2D NMR methods. *J. Am. Chem. Soc.* **134**, 12904–12907 (2012).
115. Shrot, Y. & Frydman, L. Spatially-resolved multidimensional NMR spectroscopy within a single scan. *J. Magn. Reson.* **167**, 42–48 (2004).
116. Tal, A. & Frydman, L. Spectroscopic imaging from spatially-encoded single-scan multidimensional MRI data. *J. Magn. Reson.* **189**, 46–58 (2007).
117. Schmidt, R. & Frydman, L. In vivo 3D spatial/1D spectral imaging by spatiotemporal encoding: a new single-shot experimental and processing approach. *Magn. Reson. Med.* **70**, 382–391 (2013).
118. Schmidt, R. et al. In vivo single-shot ^{13}C spectroscopic imaging of hyperpolarized metabolites by spatiotemporal encoding. *J. Magn. Reson.* **240**, 8–15 (2014).
119. Solomon, E. et al. Removing silicone artifacts in diffusion-weighted breast MRI via shift-resolved spatiotemporally encoding. *Magn. Reson. Med.* **75**, 2064–2071 (2016).
120. Jacquemmoz, C., Giraud, F. & Dumez, J.-N. Online reaction monitoring by single-scan 2D NMR under flow conditions. *Analyst* **145**, 478–485 (2020).
121. Rouger, L. et al. Ultrafast acquisition of ^{1}H–^{1}H dipolar correlation experiments in spinning elastomers. *J. Magn. Reson.* **277**, 30–35 (2017).
122. Kiryutin, A. S. et al. Ultrafast single-scan 2DNMR spectroscopic detection of a PHIP–hyperpolarized protease inhibitor. *Chem. Eur. J.* **25**, 4025–4230 (2019).
123. Gouilleux, B. et al. High-throughput authentication of edible oils with benchtop ultrafast 2D NMR. *Food Chem.* **244**, 153–158 (2018).
124. Kupče, Ē. & Sørensen, O. W. 2BOB — extracting an H2BC and an HSQC-type spectrum from the same data set, and H2OBC — a fast experiment delineating the protonated ^{13}C backbone. *Magn. Reson. Chem.* **55**, 515–518 (2017).
125. Nagy, T. M., Gyöngyösi, T., Kövér, K. E., Sørensen, O. W. & BANGO, S. E. A. XLOC/HMBC–H2OBC: complete heteronuclear correlation within minutes from one NMR pulse sequence. *Chem. Commun.* **55**, 12208–12211 (2019).
126. Bingol, K., Li, D. W., Zhang, B. & Bruschweiler, R. Comprehensive metabolite identification strategy using multiple two-dimensional NMR spectra of a complex mixture implemented in the COLMARm web server. *Anal. Chem.* **88**, 12411–12418 (2016).
127. Xella, S. et al. Embryo quality and implantation rate in two different culture media: ISM1 versus universal IVF medium. *Fertil. Steril.* **93**, 1859–1863 (2010).
128. Kupče, Ē., Kay, L. E. & Freeman, R. Detecting the afterglow of ^{13}C NMR in proteins using multiple receivers. *J. Am. Chem. Soc.* **132**, 18008–18011 (2010).
129. Kupče, Ē. & Kay, L. E. Parallel acquisition of multi-dimensional spectra in protein NMR. *J. Biomol. NMR* **54**, 1–7 (2012).
130. Marchand, J. et al. A multidimensional ^{1}H NMR lipidomics workflow to address chemical food safety issues. *Metabolomics* **14**, 60 (2018).
131. Jézéquel, T. et al. Absolute quantification of metabolites in tomato fruit extracts by fast 2D NMR. *Metabolomics* **11**, 1231–1242 (2015).
132. Pupier, M. et al. NMReDATA, a standard to report the NMR assignment and parameters of organic compounds. *Magn. Reson. Chem.* **56**, 703–715 (2018).
133. Hall, S. R. The STAR file: a new format for electronic data transfer and archiving. *J. Chem. Inf. Model.* **31**, 326–333 (1991).
134. Hall, S. R. & Spadaccini, N. The STAR file: detailed specifications. *J. Chem. Inf. Model.* **34**, 505–508 (1994).
135. Spadaccini, N. & Hall, S. R. Extensions to the STAR file syntax. *J. Chem. Inf. Model.* **52**, 1901–1906 (2012).

136. Ulrich, E. L. et al. BioMagResBank. *Nucleic Acids Res.* **36**, D402–D408 (2007).
137. Ulrich, E. L. et al. NMR-STAR: comprehensive ontology for representing, archiving and exchanging data from nuclear magnetic resonance spectroscopic experiments. *J. Biomol. NMR* **73**, 5–9 (2019).
138. Schober, D. et al. nmrML: a community supported open data standard for the description, storage, and exchange of NMR data. *Anal. Chem.* **90**, 649–656 (2018).
139. Kautz, R. A., Goetzinger, W. K. & Karger, B. L. High-throughput microcoil NMR of compound libraries using zero-dispersion segmented flow analysis. *J. Comb. Chem.* **7**, 14–20 (2005).
140. Shapira, B., Lupulescu, A., Shrot, Y. & Frydman, L. Line shape considerations in ultrafast 2D NMR. *J. Magn. Reson.* **166**, 152–163 (2004).
141. Mishkovsky, M. & Frydman, L. Interlaced Fourier transformation of ultrafast 2D NMR data. *J. Magn. Reson.* **173**, 344–350 (2005).
142. Mishkovsky, M., Kupče, Ē. & Frydman, L. Ultrafast-based projection-reconstruction 3D nuclear magnetic resonance spectroscopy. *J. Chem. Phys.* **127**, 034507 (2007).
143. Pérez-Trujillo, M., Nolis, P., Bermel, W. & Parella, T. Optimizing sensitivity and resolution in time-shared NMR experiments. *Magn. Reson. Chem.* **45**, 325–329 (2007).
144. Mobli, M. & Hoch, J. C. Nonuniform sampling and non-Fourier signal processing methods in multidimensional NMR. *Prog. Nucl. Magn. Reson. Spectrosc.* **83**, 21–41 (2014).
145. Shaka, A. J., Lee, C. J. & Pines, A. Iterative schemes for bilinear operators; application to spin decoupling. *J. Magn. Reson.* **77**, 274–293 (1988).
146. Kupče, Ē., Schmidt, P., Rance, M. & Wagner, G. Adiabatic mixing in the liquid state. *J. Magn. Reson.* **135**, 361–367 (1998).
147. Kupče, Ē. & Freeman, R. Fast multidimensional NMR by polarization sharing. *Magn. Reson. Chem.* **45**, 2–4 (2007).
148. Furrer, J. A robust, sensitive, and versatile HMBC experiment for rapid structure elucidation by NMR: IMPACT-HMBC. *Chem. Commun.* **46**, 3396 (2010).
149. Schulze-Sünninghausen, D., Becker, J. & Luy, B. Rapid heteronuclear single quantum correlation NMR spectra at natural abundance. *J. Am. Chem. Soc.* **136**, 1242–1245 (2014).
150. Spengler, N. et al. Micro-fabricated Helmholtz coil featuring disposable microfluidic sample inserts for applications in nuclear magnetic resonance. *J. Micromech. Microeng.* **24**, 034004 (2014).
151. Badilita, V. et al. On-chip three dimensional microcoils for MRI at the microscale. *Lab Chip* **10**, 1387–1390 (2010).
152. Levitt, M. H. Composite pulses. *Prog. Nucl. Magn. Reson. Spectrosc.* **18**, 61–122 (1986).
153. Khaneja, N., Reiss, T., Kehlet, C., Schulte-Herbrüggen, T. & Glaser, S. J. Optimal control of coupled spin dynamics: design of NMR pulse sequences by gradient ascent algorithms. *J. Magn. Reson.* **172**, 296–305 (2005).
154. Glaser, S. J. Unitary control in quantum ensembles: maximizing signal intensity in coherent spectroscopy. *Science* **280**, 421–424 (1998).
155. Glaser, S. J. et al. Training Schrödinger's cat: quantum optimal control. *Eur. Phys. J. D* **69**, 279 (2015).
156. Pascal, S. M., Muhandiram, D. R., Yamazaki, T., Formankay, J. D. & Kay, L. E. Simultaneous acquisition of ^{15}N- and ^{13}C-edited NOE spectra of proteins dissolved in H_2O. *J. Magn. Reson. Ser. B* **103**, 197–201 (1994).
157. Xia, Y., Yee, A., Arrowsmith, C. H. & Gao, X. $^{1}H_C$ and $^{1}H_N$ total NOE correlations in a single 3D NMR experiment. ^{15}N and ^{13}C time-sharing in t_1 and t_2 dimensions for simultaneous data acquisition. *J. Biomol. NMR* **27**, 193–203 (2003).
158. Xu, Y., Long, D. & Yang, D. Rapid data collection for protein structure determination by NMR spectroscopy. *J. Am. Chem. Soc.* **129**, 7722–7723 (2007).
159. Otikovs, M., Olsen, G. L., Kupče, Ē. & Frydman, L. Natural abundance, single-scan ^{13}C–^{13}C-based structural elucidations by dissolution DNP NMR. *J. Am. Chem. Soc.* **141**, 1857–1861 (2019).
160. Gołowicz, D., Kasprzak, P., Orekhov, V. & Kazimierczuk, K. Fast time-resolved NMR with non-uniform sampling. *Prog. Nucl. Magn. Reson. Spectrosc.* **116**, 40–55 (2020).
161. Webb, A. G. Microcoil nuclear magnetic resonance spectroscopy. *J. Pharm. Biomed. Anal.* **10**, 892–903 (2005).

Acknowledgements
L.F. acknowledges support from the Israel Science Foundation (grants 965/18) and the generosity of the Perlman Family Foundation. L.F. holds the Bertha and Isadore Gudelsky Professorial Chair and heads the Clore Institute for High-Field Magnetic Resonance Imaging and Spectroscopy, whose support is also acknowledged.

Author contributions
Introduction (A.G.W., L.F., E.K., T.D.W.C. and J.R.J.Y.); Experimentation (A.G.W., L.F., E.K., T.D.W.C. and J.R.J.Y.); Results (A.G.W., L.F., E.K., T.D.W.C. and J.R.J.Y.); Applications (A.G.W., L.F., E.K., T.D.W.C. and J.R.J.Y.); Reproducibility and data deposition (T.D.W.C. and J.R.J.Y.); Limitations and optimizations (A.G.W., L.F., E.K., T.D.W.C. and J.R.J.Y.); Outlook (A.G.W., L.F., E.K., T.D.W.C. and J.R.J.Y.); Overview of the Primer (A.G.W., L.F., E.K., T.D.W.C. and J.R.J.Y.).

Competing interests
The authors declare no competing interests.

Peer review information
Nature Reviews Methods Primers thanks M. Perez Trujillo and the other, anonymous, reviewer(s) for their contribution to the peer review of this work.

Publisher's note
Springer Nature remains neutral with regard to jurisdictional claims in published maps and institutional affiliations.

Supplementary information
The online version contains supplementary material available at https://doi.org/10.1038/s43586-021-00024-3.

RELATED LINKS
Bruker User Library: https://www.bruker.com/en/services/bruker-user-library.html
CMC-se: https://www.bruker.com/fr/products-and-solutions/mr/nmr-software/cmc-se.html